Organic & Biomolecular Chemistry

Cite this: *Org. Biomol. Chem.*, 2012, **10**, 3432

www.rsc.org/obc

PAPER

Chemiluminescence from alkoxy-substituted acridinium dimethylphenyl ester labels†

Anand Natrajan,* David Sharpe and David Wen

Received 4th January 2012, Accepted 23rd February 2012
DOI: 10.1039/c2ob00022a

Chemiluminescent acridinium dimethylphenyl ester labels are used in automated immunoassays for clinical diagnostics. Light emission from these labels is triggered by alkaline peroxide in the presence of the cationic surfactant cetyltrimethylammonium chloride (CTAC). The surfactant plays a critical role in the chemiluminescence process of these labels by both accelerating their emission kinetics and increasing total light output enabling high throughout and improved assay sensitivity in automated immunoassays. Despite the surfactant's crucial role in the chemiluminescent reaction, no study has investigated how structural perturbations in the acridinium ring could impact the influence of the surfactant. We describe herein the synthesis and properties of three new alkoxy-substituted, acridinium dimethylphenyl esters where the nature of the alkoxy group in the acridinium ring was varied (hydrophobic or hydrophilic). Chemiluminescence measurements of these alkoxy-substituted labels indicate that hydrophilic functional groups in the acridinium ring, in particular sulfobetaine zwitterions, disrupt surfactant-mediated compression of emission times but not enhancement of light yield. These results support the hypothesis that surfactant-mediated effects require the binding of two different reaction intermediates to surfactant aggregates and, that surfactants influence light emission from acridinium esters by two separate mechanisms. Our studies also indicate that preservation of both surfactant effects on acridinium ester chemiluminescence and low non-specific binding of the label can be achieved with a relatively hydrophobic acridinium ring coupled to a hydrophilic phenolic ester leaving group.

Introduction

Chemiluminescent acridinium dimethylphenyl esters (**9d** and **10d**, Fig. 1) are used as labels for clinical diagnostic immunoassays in automated instruments.[1] These acridinium esters are used to label proteins such as antibodies, antigens or small analytes and, the labeled reagents are used in conjunction with magnetic microparticles for sensitive analytical measurements of a wide range of clinically important analytes. At the end of the assay, light emission from the acridinium ester label is triggered by the sequential addition of two reagents. An initial addition of 0.1 M nitric acid containing 0.5% hydrogen peroxide is followed by the addition of 0.25 M sodium hydroxide containing the cationic surfactant cetyltrimethylammonium chloride (CTAC). At neutral pH, most acridinium esters exist as the water-adduct **i** (Fig. 2) commonly referred to as the pseudobase[2] which cannot participate directly in the chemiluminescent reaction. The acid treatment restores the electrophilic center at C-9 by rapidly converting the pseudobase to the acridinium ester **ii** (Fig. 2). Subsequent addition of base ionizes the hydrogen peroxide and initiates the chemiluminescent process. Hydroperoxide ion addition to C-9 forms the adduct **iii** which eventually leads to the formation of the primary emitter, excited state acridone **vi**. Dioxetanone **v** has been proposed as an intermediate in this process[3] but detailed theoretical studies[4] have suggested that direct formation of the excited state acridone **vi** from dioxetane **iv** is energetically favored.

In a recent study, we reported that micelles of cationic surfactants such as CTAC play a critical role in the chemiluminescence of acridinium dimethylphenyl ester labels (containing unsubstituted *N*-sulfopropylacridinium rings) and their conjugates.[1d] The surfactant not only compressed emission times from approximately one minute in the absence of surfactant to <5 seconds but, was also observed to increase total light output by 3–4 fold. We attributed the acceleration in emission kinetics to increased local concentration of hydroperoxide ions at the surface of CTAC aggregates which should facilitate formation of the peroxide adduct **iii** (Fig. 2). Similar enhancements in observed rates have also been reported in other bimolecular reactions such as ester hydrolysis by hydroperoxide ions in the presence of cetyltrimethylammonium micelles.[5] To explain the effect of the

Siemens Healthcare Diagnostics, Advanced Technology and Pre-Development, 333 Coney Street, East Walpole, MA 02032, USA. E-mail: anand.natrajan@siemens.com; Fax: +1-508-660-4591; Tel: +1-508-660-4582

†Electronic supplementary information (ESI) available: See DOI: 10.1039/c2ob00022a

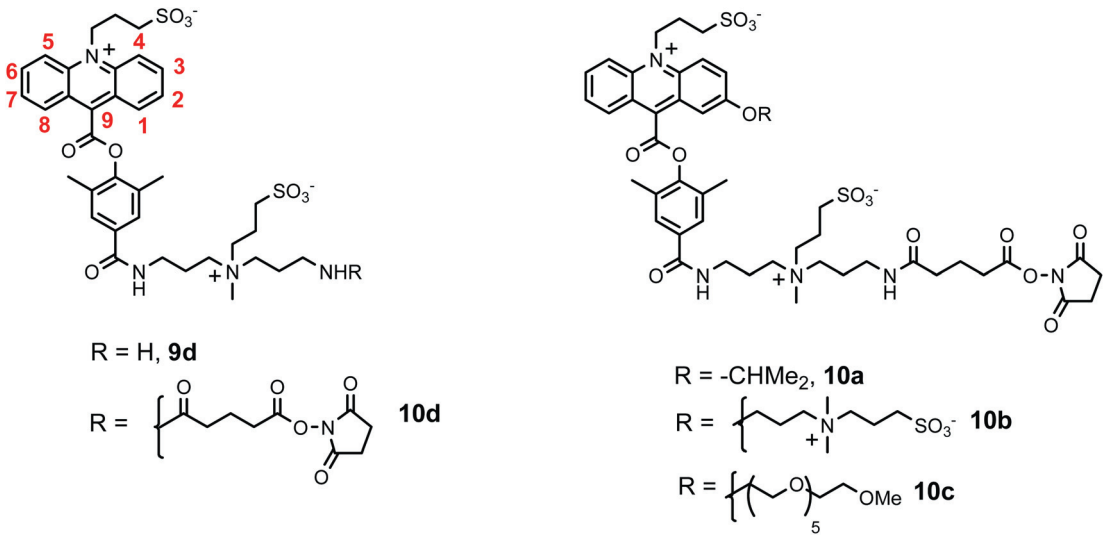

Fig. 1 Structures of zwitterionic acridinium esters.

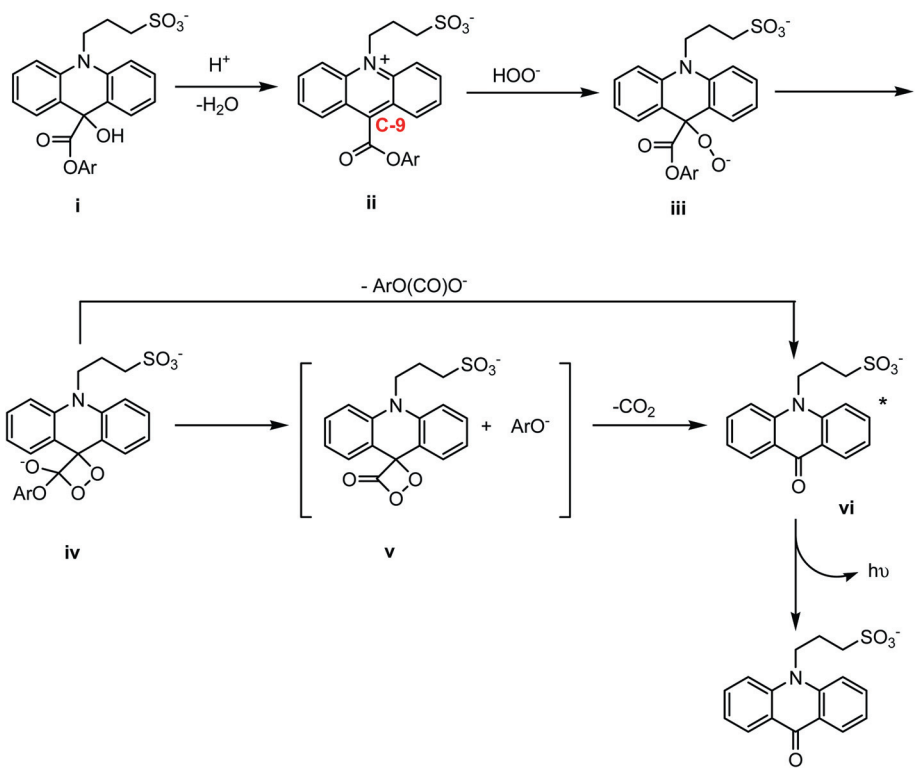

Fig. 2 Simplified reaction pathway of chemiluminescence from *N*-sulfopropyl acridinium esters.[1d] Cationic surfactants influence conversion of **ii** to **iii** by increasing the local concentration of hydroperoxide ions. Surfactants also facilitate formation of dioxetane **iv** from **iii** by offering a lower polarity medium for this intramolecular cyclization reaction that involves dispersal of negative charge in the transition state.

surfactant in significantly increasing light output, we proposed that the lower polarity of the micellar medium would be conducive to the formation of the critical dioxetane intermediate **iv** from intramolecular cyclization of **iii**. This reaction involves dispersal of negative charge in the transition state and classical Hughes–Ingold theory[6] predicts that a lower polarity medium would lower the activation energy of the reaction. In fact, our proposal was based on analogous micellar effects that have been reported in detailed studies of unimolecular reactions such as the intramolecular cyclization reactions of *ortho*-haloalkyl-substituted phenoxides, decarboxylation of 6-nitrobenzisoxazole-3-carboxylate and, 1,2-elimination reactions.[7,8] All these reactions involve dispersal of negative charge in their transition states and, are catalyzed by aggregates of cationic and zwitterionic surfactants because of reduced polarity (alcohol-like) at the micellar phase.[7,8]

Solute binding to ionic micelles such as those of cetyltrimethylammonium salts results from a combination of hydrophobic and Coulombic interactions.[9] Given the critical role of the surfactant in the chemiluminescence of acridinium dimethylphenyl esters, any useful structural alteration of acridinium ester must ensure that the surfactant's influence is not disrupted. Based on the chemiluminescence mechanism outlined in Fig. 2, strong binding of the acridine ring in the acridinium ester **ii** and the peroxide adduct **iii**, to surfactant aggregates is crucial to observe the effect of the surfactant on the chemiluminescence process *i.e.* acceleration of emission kinetics and enhanced light output. However, these requirements pose an interesting dilemma. In immunoassays that use microparticles and fluorescent or chemiluminescent labels, high non-specific binding, attributable to label hydrophobicity and/or charge often limits assay sensitivity.[1a] Is there a way to reconcile these seemingly contradictory requirements in the design of new acridinium ester labels so that the critical influence of the surfactant on the chemiluminescence process is retained without exacerbating the non-specific binding of the labels? We report herein a study aimed to answer this question as well as to outline some general principles that, until now, have been lacking, for the design of acridinium dimethylphenyl ester labels that not only exhibit fast light emission and high light output in the presence of surfactants but, also display low non-specific binding to magnetic microparticles. Our conclusions are based on the study of the chemiluminescence of new, C-2 alkoxy-substituted, acridinium ester labels (Fig. 1), where the nature of the alkoxy group was varied (hydrophobic or hydrophilic). Our results on chemiluminescence measurements of these labels also lend further support to the hypothesis that surfactants influence light emission from acridinium dimethylphenyl ester labels by two discrete mechanisms.

Results and discussion

Synthesis of C-2 alkoxy-substituted, zwitterionic acridinium esters and protein conjugates

To study the effect of structural perturbation of the acridinium ring on the chemiluminescence reaction both in the presence and absence of surfactants, we elected to synthesize three different, C-2 alkoxy-substituted acridinium dimethylphenyl ester labels (**10a–10c**, Fig. 1). Acridinium esters with methoxy groups at C-2 and/or C-7 (see Fig. 1 for numbering system) display enhanced light output but poor chemiluminescence stability[1a] and, in the current study, we wanted to optimize the structure of the alkoxy group not only for fast light emission and maximum light output in the presence of surfactants but also for good chemiluminescence stability and low non-specific binding. Reducing the bulk of the label and synthetic complexity were other important objectives that we wanted to achieve. The phenolic oxygen at C-2 on the acridine ring provided a convenient handle to attach different functional groups using a common synthetic precursor (compound **5** in Fig. 3). A C-2 isopropyloxy group was selected as representative of a relatively hydrophobic substituent (**10a**, Fig. 1). For hydrophilic functional groups, two non-ionic alkoxy groups were selected, one containing a highly polar sulfobetaine zwitterion (**10b**) and the other containing the poly(ethylene) glycol (PEG) derivative, methoxy(hexaethylene) glycol (**10c**). To ensure aqueous solubility of all three, alkoxy-substituted acridinium esters, a hydrophilic linker containing a sulfobetaine zwitterion, disclosed previously,[1d] was incorporated *para* to the phenolic ester leaving group as illustrated in Fig. 1. The structures illustrated in Fig. 1 can be classified in simple terms, while referring to the acridinium ring and the phenolic ester with the sulfobetaine linker respectively as, hydrophobic–hydrophilic (**10a**) and hydrophilic–hydrophilic (**10b** and **10c**). Compound **10d**, with an unsubstituted acridinium ring was described previously[1d] and contains a relatively hydrophobic acridinium ring along with a hydrophilic phenolic ester leaving group.

The synthetic scheme for compounds **10a–10c** is shown in Fig. 3. Synthesis of the common intermediate 2-hydroxyacridine ester **5** was accomplished in five steps starting with commercially available isatin **1**. *N*-Arylation of isatin **1** with 4-bromoanisole in the presence of copper(I) iodide was followed by rearrangement of the crude *N*-arylisatin derivative to 2-methoxyacridine-9-carboxylic acid **2** in refluxing base.[10] Although the overall yield of this two step process was modest (43%), the reaction was amenable to scale up and the acridine carboxylic acid **2** could be isolated without chromatography. Esterification of 2-methoxyacridine carboxylic acid **2** with methyl 4-hydroxy-3,5-dimethylbenzoate **3** in the presence of *p*-toluenesulfonyl chloride in pyridine afforded the C-2 methoxy-substituted acridine ester **4** in 86% yield after purification by chromatography on silica. Cleavage of the methyl ether in **4** was carried out using boron tribromide in dichloromethane which also cleaved the methyl ester. However, during the process of quenching excess boron tribromide with cold methanol, the methyl ester was reinstalled to give compound **5** in 90% isolated yield following purification on silica.

With compound **5** in hand, we used the Mitsunobu reaction[11] to install the requisite aryl ether linkages in compounds **6a–6c**. Thus, treatment of compound **5** with 2-propanol, 3-dimethylamino-1-propanol and methoxy(hexaethylene) glycol in the presence of triphenylphosphine and diisopropylazodicarboxylate (DIAD) afforded the alkoxy-substituted acridine esters **6a**, **6b** and **6c** respectively. Isolated yields of **6a** and **6b** were high ≥ 80% whereas **6c** was isolated in modest (38%) yield. Conversion of the alkoxy-substituted acridine esters **6a–6c** to the *N*-sulfopropyl acridinium esters was accomplished by *N*-alkylation of the acridine nitrogen with 1,3-propane sultone in the ionic liquid 1-butyl-3-methylimidazolium hexafluorophosphate [BMIM][PF_6]. We reported previously that ionic liquids are excellent media for the *N*-alkylation of the hindered nitrogen of acridine esters with 1,3-propane sultone[12] and, we now routinely use this protocol for a variety of acridine ester substrates. In the case of substrate **6b**, both the acridine nitrogen as well as the dimethylamino group were *N*-alkylated in one step in excellent (~80%) conversion as judged by HPLC analysis. The *N*-sulfopropyl acridinium methyl ester intermediates were directly hydrolyzed to the acridinium carboxylic acids **7a–7c** and subsequently purified by preparative HPLC. Conversion to the final targets **10a–10c** first entailed addition of the zwitterionic sulfobetaine linker **8**[1d] to the carboxylic acids in **7a–7c** using *N*-hydroxysuccinimide (NHS) ester chemistry for carboxylate activation. The amine-containing, zwitterionic acridinium esters **9a–9c** were converted to the targets **10a–10c** by first condensing with glutaric anhydride

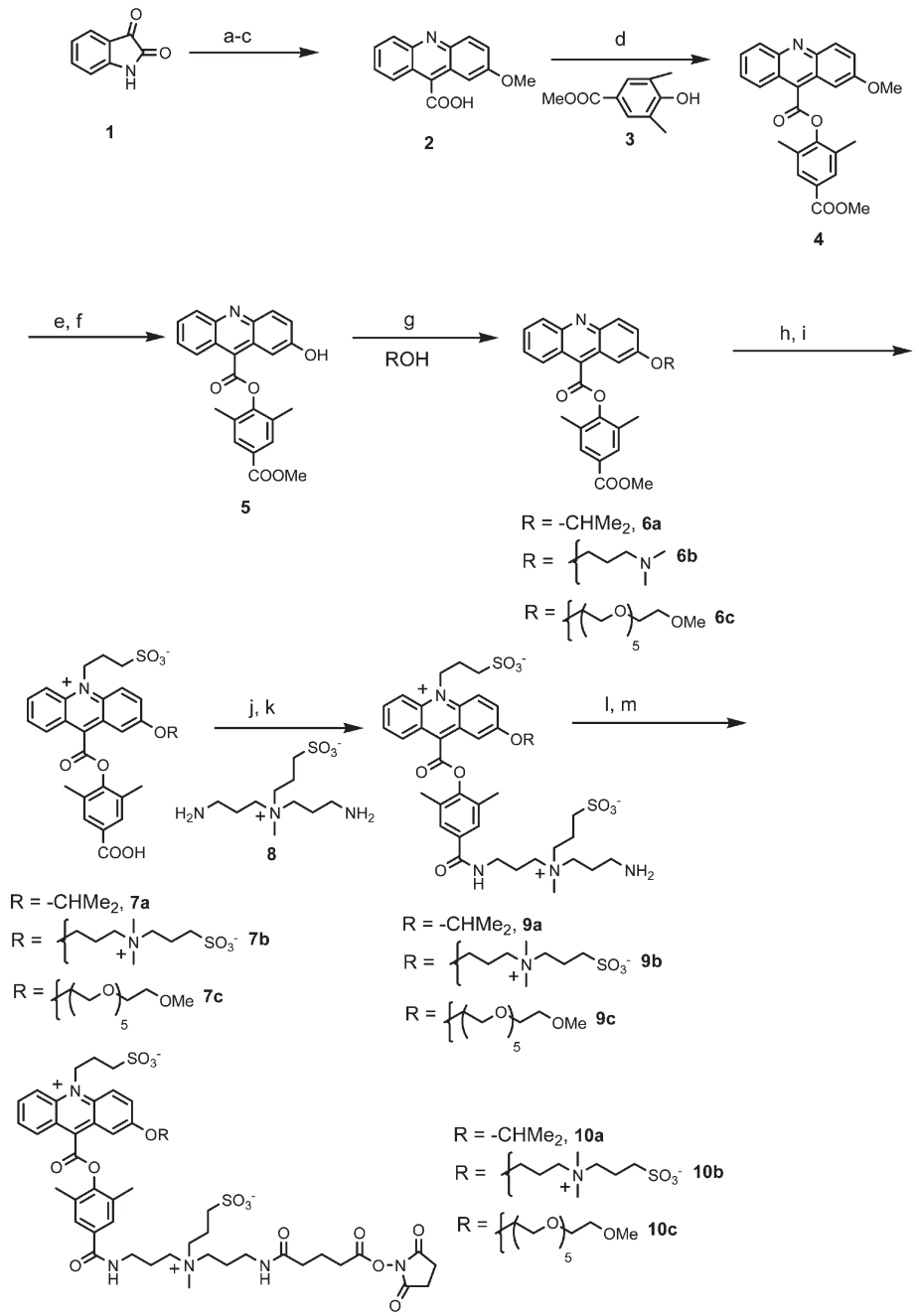

Fig. 3 Synthetic scheme for C-2, alkoxy-substituted, acridinium esters. Reagents: (a) sodium hydride, DMF; (b) 4-bromoanisole, copper(I) iodide, DMF; (c) 10% potassium hydroxide; (d) *p*-toluenesulfonyl chloride, pyridine; (e) boron tribromide, dichloromethane; (f) methanol; (g) diisopropyl azodicarboxylate, triphenylphosphine, THF; (h) 1,3-propane sultone, 2,6-di-*tert*-butylpyridine, 1-butyl-3-methylimidazolium hexafluorophosphate; (i) 1 N HCl; (j) *N*,*N*,*N*′,*N*′-tetramethyl-*O*-(*N*-succinimidyl)uronium tetrafluoroborate (TSTU), diisopropylethylamine, DMF; (k) 0.25 M sodium bicarbonate, DMF (l) glutaric anhydride, diisopropylethylamine, methanol; (m) TSTU, diisopropylethylamine, DMF–water.

followed by conversion of the glutarate derivatives to the NHS esters.

HPLC analyses of all the intermediates and final compounds of Fig. 3 are shown in the ESI† (Fig. S1–S16†).

Protein conjugates of compounds **10a–10c** were prepared using a murine anti-TSH (thyroid stimulating hormone) monoclonal antibody as described in the Experimental section. Label incorporation was measured by mass spectroscopy which indicated a similar level of label incorporation of approximately 4 labels per antibody molecule using 7.5–10 equivalents input of compounds **10a–10c** in the labeling reactions.

Emission spectra and pseudobase formation

Acridinium esters with electron-donating methoxy groups at C-2 and/or C-7 of the acridinium ring display bathochromic shifts in their emission spectra compared to unsubstituted acridinium

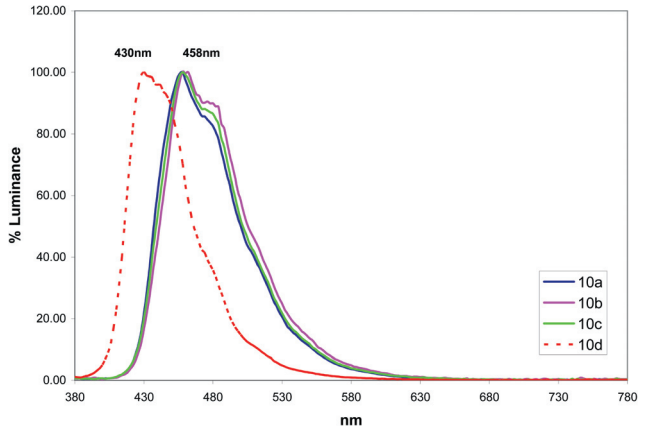

Fig. 4 Emission spectra of acridinium esters. Compounds **10a**, **10b**, and **10c** with C-2 alkoxy groups exhibit a shift in the emission wavelength maximum to 458 nm compared to 430 nm for the unsubstituted acridinium ester **10d**.

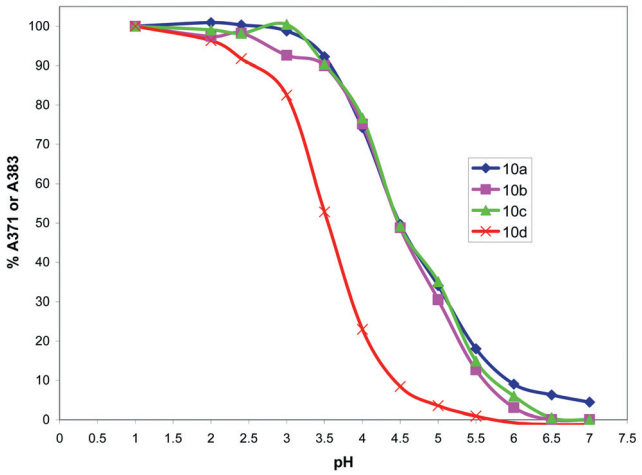

Fig. 5 pH Titrations of acridinium esters illustrating conversion of the acridinium form **ii** to the pseudobase **i**. Compounds **10a**, **10b**, and **10c** with C-2 alkoxy groups exhibit a shift in the pK_a to 4.5 from 4.0 for the unsubstituted acridinium ester **10d**.

esters.[1a] A single C-2 methoxy group was observed to shift the emission maximum to 458 nm compared to 426 nm for an unsubstituted acridinium ester.[1a] Emission spectra (Fig. 4) of the alkoxy-substituted acridinium esters **10a–10c** were recorded using a spectral camera to determine whether there are any differences in the emission spectra of these compounds caused by the different alkoxy groups. As illustrated in Fig. 4, all three compounds **10a–10c** emitted light with spectral maxima centered at 458 nm. In comparison, compound **10d**, with an unsubstituted acridinium ring, exhibited an emission maximum centered at 430 nm. These results suggest that the electron donating ability of the C-2, aryl ether oxygen in compounds **10a–10c** is not affected by structural differences in the alkoxy functional groups.

Another characteristic of acridinium esters that is a reflection of the electronics of the acridinium ring is the pH of pseudobase formation from the addition of water to C-9 (formation of **i** from **ii** in Fig. 2). As reported previously by Bunting *et al.*,[13] acridinium cations, at low pH, display a strong absorption band at approximately 360 nm that disappears as the pH is raised due to disruption of the acridinium ring chromophore caused by addition of hydroxide ion to C-9. UV-Visible spectra of compounds **10a–10d** at low pH (pH = 2.8) and the corresponding amines **9a–9d** at high pH (pH = 9) are shown in Fig. S17–S20 (ESI†) and, they illustrate the absorption bands of the acridinium forms of these compounds and their corresponding pseudobases. (The amine derivatives **9a–9d** were used at pH 9 to avoid NHS ester hydrolysis in **10a–10d**.) As can be noted from the spectra, the acridinium forms of the compounds **10a–10c**, containing C-2 alkoxy groups, displayed strong absorption bands centered at 383 nm whereas compound **10d** with an unsubstituted acridinium ring, displayed the same absorption band at 371 nm. At pH 9, this long wavelength absorption band was bleached for all compounds because they exist predominantly as the pseudobase. Titration of the acridinium chromophore as a function of pH is thus a convenient way to measure the pK_a of the acridinium to pseudobase transition of acridinium esters.

Titration of the acridinium chromophore of compounds **10a–10d** as a function of pH (pH range 1–7) is illustrated in Fig. 5. Electron-donating groups at C-2 and/or C-7 of the acridinium ring should reduce the electrophilic character of C-9 and shift the pH of pseudobase formation to more basic pH. This prediction is indeed borne out for all three alkoxy-substituted compounds **10a–10c** that exhibited a pK_a of 4.5 for conversion of the acridinium forms to their corresponding pseudobases. Compound **10d** had a more acidic pK_a of 4.

Identical chemiluminescence emission spectra, UV-Visible spectra and pK_a of pseudobase formation of compounds **10a–10c** indicate that the different alkoxy groups in these compounds have very similar effects on the electronics of the acridinium ring.

Chemiluminescence measurements

Chemiluminescence measurements of the alkoxy-substituted labels **10a–10c** as well their anti-TSH antibody conjugates were carried out as described previously for compound **10d** and its conjugates[1d] both in absence and presence of surfactants. In a typical experiment, 1–2 mg mL^{-1} solutions of HPLC-purified labels **10a–10c** and the corresponding protein conjugates of these compounds were serially diluted in phosphate buffer to approximately 0.5 nM (nm = nanomolar, 10^{-9} M) for the free labels and, approximately 0.2 nM for the protein conjugates as described in the Experimental section. Chemiluminescence from 0.01 mL of each diluted sample was triggered by the addition of 0.3 mL each of 0.1 M nitric acid containing 0.5% (~80 mM) hydrogen peroxide followed by the addition of 0.25 M sodium hydroxide. Light was collected for a total of two minutes, integrated at 0.5 second intervals, using a luminometer. The light collection time was sufficiently long for complete emission under all conditions. In experiments involving surfactants, the surfactant was included in the second reagent (0.25 M sodium hydroxide) at five times its reported critical micelle concentration (CMC) in water. The surfactants selected for the current study were two cationic surfactants cetyltrimethylammonium chloride (CTAC) and cetyltripropylammonium chloride (CTPAC), as well as the sulfobetaine surfactant *N*,*N*-dimethyldodecylammonio-

Table 1 Time (seconds[a]) for emission of >90% total light of alkoxy-substituted acridinium ester labels in the absence and presence of surfactants

Compound	No surfactant	CTAC[b]	CTPAC[b]	DDAPS[b]
10a	52.5	1.0	1.0	3.5
10b	55	17.5	19.0	29.0
10c	41.5	1.5	3.5	18.0

[a] Average of three replicates. [b] Abbreviations used: CTAC = cetyltrimethylammonium chloride (cationic), CTPAC = cetyltripropylammonium chloride (cationic), DDAPS = *N*,*N*-dimethyldodecylammonio-1,3-propane sulfonate (zwitterionic).

Table 2 Time (seconds[a]) for emission of >90% total light of anti-TSH antibody conjugates of alkoxy-substituted acridinium ester labels in the absence and presence of surfactants

Conjugate	No surfactant	CTAC	CTPAC	DDAPS
Anti-TSH-**10a**	40.5	1.0	1.0	4.5
Anti-TSH-**10b**	47.5	14.5	14.5	27.5
Anti-TSH-**10c**	37.5	1.0	2.0	7.5

[a] Average of three replicates.

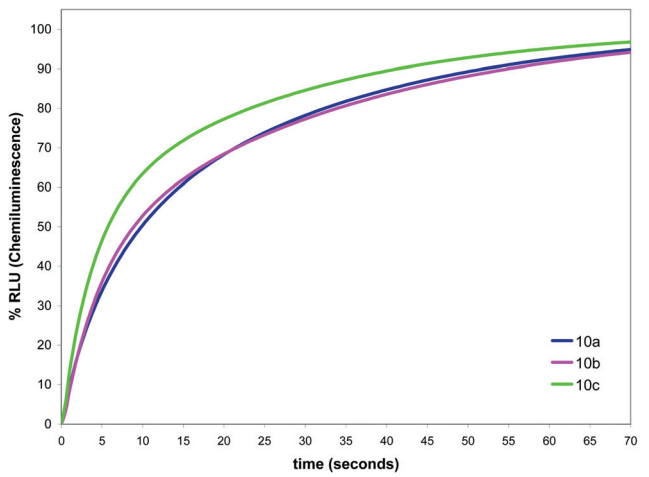

Fig. 6 Chemiluminescence profiles of alkoxy-substituted acridinium esters in the absence of surfactant.

1,3-propane sulfonate (DDAPS). In our previous study[1d] these surfactants afforded the greatest impact on the chemiluminescence of unsubstituted acridinium esters and their conjugates.

The effect of the three surfactants on the emission times of the alkoxy-substituted acridinium ester labels **10a–10c** and their corresponding anti-TSH antibody conjugates are illustrated in Tables 1 and 2. These emission times reflect the ability of the surfactant in accelerating light emission. The emission profiles of the labels **10a–10c** are shown in Fig. 6–9 and those of the anti-TSH antibody conjugates, which were similar, are shown in Fig. S21–S24 (ESI†).

As can be noted from Tables 1 and 2, in the absence surfactant light emission was observed to be quite slow for both the free labels and the protein conjugates. Although the protein conjugates showed marginally faster light emission, yet emission times for the emission of >90% of total light required >35 seconds. These results are similar to what we observed previously for unsubstituted acridinium esters.[1d] In the presence of the two cationic surfactants CTAC and CTPAC, light emission

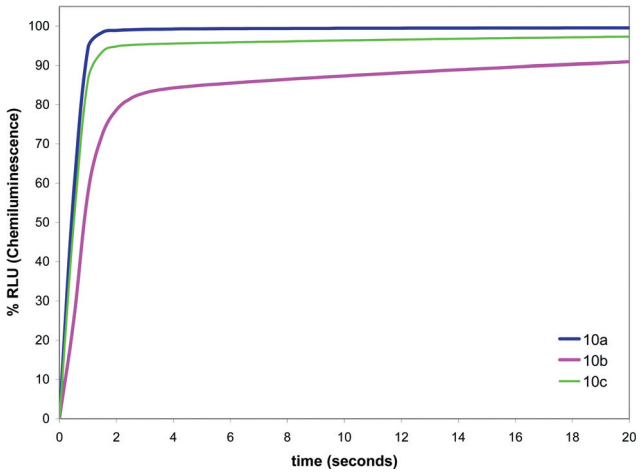

Fig. 7 Chemiluminescence profiles of alkoxy-substituted acridinium esters in the presence of the cationic surfactant CTAC.

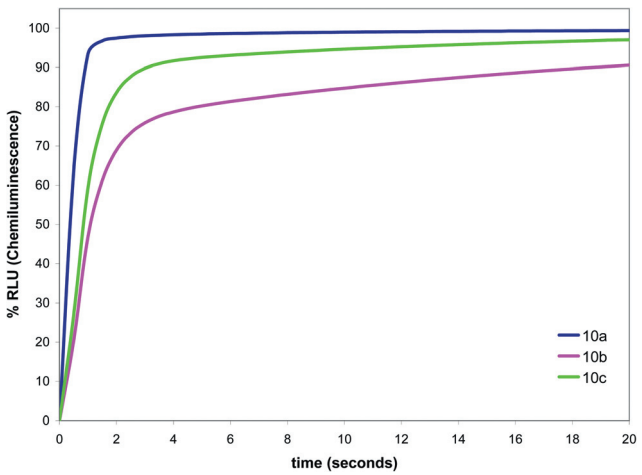

Fig. 8 Chemiluminescence profiles of alkoxy-substituted acridinium esters in the presence of the cationic surfactant CTPAC.

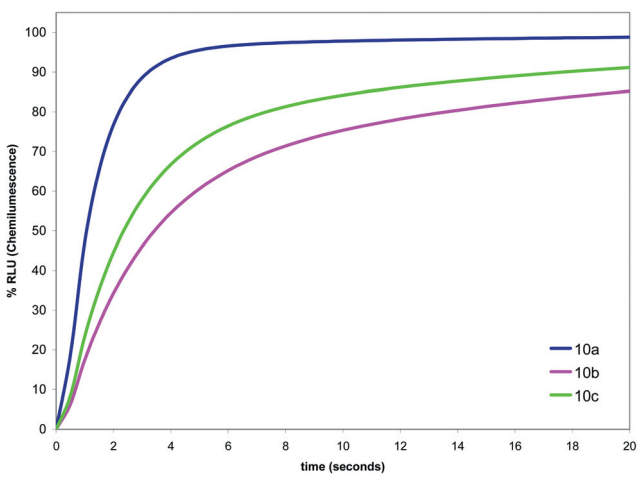

Fig. 9 Chemiluminescence profiles of alkoxy-substituted acridinium esters in the presence of the zwitterionic surfactant DDAPS.

Table 3 Specific activity (RLUs[a] per mole × 10^{-19}) of alkoxy-substituted acridinium ester labels at a measurement time of 2 min. Values in parentheses reflect the enhancement in light output in the presence of surfactant

Compound	No surfactant	CTAC	CTPAC	DDAPS
10a	2.0	8.4 (4.2)	10.3 (5.0)	10.0 (5.0)
10b	1.8	6.1 (3.4)	6.9 (3.8)	5.4 (3.0)
10c	2.4	7.7 (3.2)	9.3 (3.9)	6.6 (2.8)

[a] RLU = relative light unit.

Table 4 Specific activity (RLUs per mole × 10^{-19}) of anti-TSH antibody conjugates of alkoxy-substituted acridinium ester labels at a measurement time of two minutes. Values in parenthesis reflect the enhancement in light output in the presence of surfactant

Conjugate	No surfactant	CTAC	CTPAC	DDAPS
Anti-TSH-**10a**	1.7	7.1 (4.2)	8.1 (4.8)	8.0 (4.7)
Anti-TSH-**10b**	1.2	4.1 (3.4)	4.3 (3.6)	3.6 (3.0)
Anti-TSH-**10c**	2.2	7.4 (3.4)	7.9 (3.6)	6.1 (2.8)

from **10a** and **10c** and their antibody conjugates was significantly faster and the emission times were compressed to <5 seconds. On the other hand, the label **10b** and its protein conjugate, showed a less dramatic acceleration of emission kinetics even in the presence of these cationic surfactants. Acceleration of emission kinetics was also attenuated in micelles of the zwitterionic surfactant DDAPS for all labels as well as their protein conjugates. However, emission kinetics of the acridinium label **10a** with a more hydrophobic ring was less severely affected compared to **10b** and **10c** which have more hydrophilic acridinium rings.

The effect of the three surfactants on total light output of the alkoxy-substituted acridinium ester labels **10a–10c** and their corresponding anti-TSH antibody conjugates are illustrated in Tables 3 and 4. In Tables 3 and 4, light output for each label is presented as specific activity in units of RLUs per mole (RLU = relative light unit). The specific activity values in Tables 3 and 4 reflect the ability of the three surfactants in increasing total light yield from the acridinium ester labels and their protein conjugates.

In the absence of surfactant, the three labels **10a–10c** showed depressed light output but the specific activity was similar for all three labels. These results indicate that structural differences in the alkoxy groups in these labels have little impact on the chemiluminescent reaction. For protein conjugates (Table 4), a similar result was observed except for the conjugate of label **10b** which had slightly lower specific activity compared to **10a** and **10b**. Total light output in the presence of the three surfactants was enhanced for all three labels to a similar extent. Compound **10a** in particular, which has a more hydrophobic acridinium ring, showed an enhancement in light output of 4–5-fold in the presence of all three surfactants. Enhancement was also higher in the presence of micelles of CTPAC and DDAPS which are less polar than CTAC micelles.[7d] Enhancement in light output was slightly attenuated (3–4-fold) for **10b** and **10c** with hydrophilic acridinium rings both for free labels as well as the protein conjugates.

The results in Tables 1–4 prompts the following question: why are surfactants equally effective in enhancing light output of acridinium ester labels with hydrophobic (**10a**) and hydrophilic acridinium rings (**10b** and **10c**) but, are significantly less effective in accelerating emission kinetics of the latter (especially **10b**)?

Micellar catalysis of bimolecular reactions results from increased local concentrations of the reactants in a small volume of the micellar phase.[14] Cationic micelles in particular can bind negatively charged ions such as hydroperoxide ions and, provide a high local concentration of these reactive ions to micelle-bound substrates. For zwitterionic micelles, this ion binding is weaker.[15] Micelles also provide a low polarity (alcohol-like) environment that facilitates unimolecular reactions whose transition states involve charge dispersal.[7,8] For these unimolecular reactions, the magnitude of the catalysis has been observed to be greater in less polar micelles derived from CTPAC and DDAPS.[7,8] Substrate binding to ionic micelles is through a combination of hydrophobic and charge interactions. In an elegant study, Bunton and Sepulveda[9a] examined the binding of a series of phenol derivatives of increasing hydrophobicity to cetyltrimethylammonium bromide (CTAB) micelles at both low and high pH. At low pH, where the phenols were uncharged, the magnitude of the binding to CTAB micelles increased with increasing hydrophobicity of the phenol. At high pH, where the phenols were ionized to the phenoxides, binding for each phenol analog was significantly stronger compared to its unionized counterpart.

Based on the chemiluminescence reaction pathway of acridinium esters outlined in Fig. 2, acceleration of emission kinetics requires efficient binding of the acridinium esters **ii** to surfactant aggregates whereas increase in light output requires binding of the peroxide adduct **iii**. An examination of the structural features of the acridine rings of **ii** and **iii** indicate some crucial differences that can affect their binding to micelles. The acridinium esters **ii** contain no net charge and consequently binding to micelles is expected to be primarily through hydrophobic interactions of the acridinium ring with the surfactant. On the other hand, the acridine ring of the peroxide adduct **iii** contains two negative charges. Binding of this reaction intermediate to cationic and zwitterionic micelles is expected to be much stronger due to both hydrophobic and charge interactions. The relatively weaker interaction of the acridinium ring of **ii** with surfactants is expected to be more easily disrupted by the introduction of hydrophilic functional groups in the acridinium ring. Our results with label **10b** which, has a very polar sulfobetaine zwitterion in the acridinium ring, indicates that this is indeed the case. This label showed relatively slow light emission even in the presence of cationic surfactants. The label **10c** also contains a hydrophilic acridinium ring but with a different functional group PEG, that structurally is very similar to the non-ionic surfactant triton X-100. The latter surfactant exhibits ideal mixing with cationic surfactants,[16] which suggests that PEG introduction in the acridinium ring is not likely to be as disruptive to binding to cationic micelles. Chemiluminescence measurements of label **10c** are consistent with this expectation. Finally, because the acridine ring of peroxide adduct **iii** (Fig. 2) of all three labels **10a–10c** is negatively charged, augmentation of hydrophobic binding with significant charge interactions should result in minimal

Table 5 Partition coefficients of acridinium ester labels to CTAC micelles (K_{MW}) and to the HPLC stationary phase (K_{SW})

Compound, K_{MW} (pH 2.8)	Compound, K_{SW} (pH 2.8)	Compound, K_{MW} (pH 9)	Compound, K_{SW} (pH 9)
10a, 578	**10a**, 30	**9a**, $(>10^4)^a$	**9a**, —
10b, —	**10b**, —	**9b**, 3433	**9b**, 141
10c, 103	**10c**, 5	**9c**, 1895	**9c**, 58
10d, 3486	**10d**, 256	**9d**, $(>10^4)^a$	**9d**, —

[a] Estimated. K_{MW} of **10b** was too weak to measure by HPLC.

disruption in the influence of the surfactant on light yield even for acridinium esters with hydrophilic acridinium rings. Consistent with this prediction, we observed similar enhancement in light output for all three labels **10–10c** and their protein conjugates in the presence of surfactants.

Micelle–water partition coefficients

To provide support for our proposals that two different reaction intermediates (**ii** and **iii** in Fig. 2) bind with differing strengths to surfactant aggregates, we measured micelle–water partition coefficients (K_{MW}) of the alkoxy-substituted acridinium esters (**10a–10d** and **9a–9d**) to CTAC micelles. Peroxide adduct **iii** is an unstable reaction intermediate and therefore we used the pseudobase adduct **i** of the amine derivatives **9a–9d** to simulate its binding to CTAC micelles at pH = 9. At this pH, compounds **9a–9d** exist solely as the pseudobase (Fig. 5 and Fig. S17–S20†). Binding of the acridinium esters **10a–10d** to CTAC micelles was measured at pH 2.8. At this pH, the compounds exist predominantly in the acridinium form as can be noted from Fig. 5 and Fig. S17–S20.† The amine derivatives **9a–9d** also do not contain any charge in the phenolic ester leaving group at pH = 9. Similarly, the NHS esters **10a–10d**, have a charge-neutral leaving group at pH = 2.8. Thus, any observed differences in binding for these compounds to CTAC micelles can be attributed mainly to structural differences (hydrophobicity and charge) in their acridine rings.

We used a chromatographic (HPLC) method pioneered by Armstrong and Nome[17] for the measurement of partition coefficients of the acridinium esters to CTAC micelles as described in the ESI.† Micelle–water partition coefficients (K_{MW}) of acridinium esters **10a–10d** and the corresponding amine derivatives **9a–9d** to CTAC micelles are listed in Table 5. For the acridinium esters, at pH 2.8, K_{MW} decreased in the order **10c** < **10a** < **10d**. As predicted, the acridinium esters with the more hydrophobic rings (**10a** and **10d**) partitioned more strongly than acridinium esters with hydrophilic acridinium rings (**10c**). Compound **10b**, containing a very hydrophilic acridinium ring with a sulfobetaine zwitterion, showed poor retention on the HPLC column which also did not change as a function of surfactant concentration. Micelle binding of this compound thus appears weak which is consistent with chemiluminescence measurements that showed only marginal acceleration in emission kinetics in the presence of CTAC.

The pseudobases of the amine derivatives **9a–9d** contain negatively charged acridine rings and as a result, micelle–water partition coefficients for all compounds were observed to be

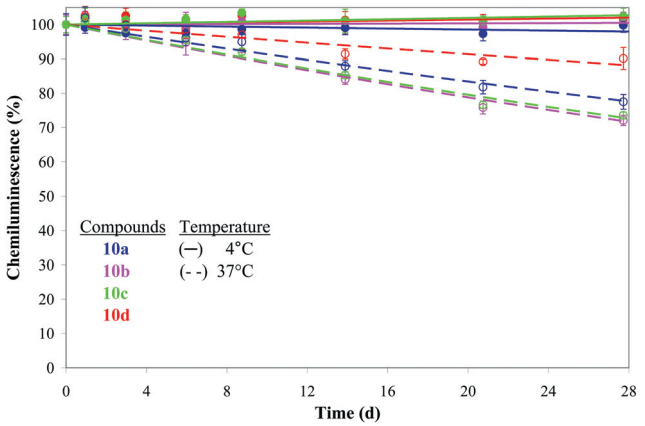

Fig. 10 Chemiluminescence stability of anti-TSH antibody conjugates of acridinium ester labels in pH 8 buffer at 4 °C and 37 °C. Order of decreasing stability at 37 °C are **10d** > **10a** ≥ **10c** = **10b**. Alkoxy-substituted acridinium ester conjugates were marginally less stable at 37 °C but were equally stable at 4 °C after 4 weeks.

significantly greater. In contrast to the weak binding observed at low pH, the acridinium ester with a polar sulfobetaine zwitterion in the acridinium ring (**9b**) showed strong partitioning into CTAC micelles. A similar result was observed for compound **9c** whose K_{MW} at pH = 9 was approximately 20-fold higher compared to pH 2.8. The two acridinium esters, **9a** and **9d**, with hydrophobic acridinium rings showed very strong partitioning into CTAC micelles at pH 9. Partition coefficient plots (Fig. S28 and S31†) of these compounds actually had negative intercepts. Partition coefficients for these two compounds could not be accurately estimated but appear to be $>10^4$. The acridine ring of peroxide intermediate **iii** (Fig. 2) contains two negative charges and micelle binding is expected to be even stronger for this reactive intermediate for all labels. In conclusion, our observations on micellar partitioning of acridinium esters and their corresponding pseudobases indicate that charge interactions can compensate for weak hydrophobic binding. Thus, the micelle's role in enhancing light yield is only marginally affected for labels with hydrophilic acridinium rings.

Chemiluminescence stability and non-specific binding

For practical applications, such as in clinical immunoassays, acridinium ester labels must have low non-specific binding (a requisite for assay sensitivity) and, must exhibit good chemiluminescence stability (necessary for long shelf life of reagents).

Chemiluminescence instability of acridinium esters is mostly attributed to hydrolysis of the phenolic ester linkage,[2] but the introduction of two, flanking methyl groups dramatically improves the stability of the phenolic ester.[18] The chemiluminescence stability of the anti-TSH antibody conjugates of the four labels **10a–10d** at 4 °C and at 37 °C in pH = 8 buffer is shown in Fig. 10. As can be noted from the figure, the four labels showed no loss of chemiluminescence even after 28 days at 4 °C. Increasing the temperature to 37 °C showed the loss of a small amount (10–20%) of chemiluminescence for all labels in the same timeframe. The alkoxy-substituted acridinium ester labels **10a–10c** were more or less equally stable at this

temperature. Because the C-2 alkoxy groups are remote from the phenolic ester linkage, structural variations in these alkoxy groups in **10a–10c** are not expected to and did not affect chemiluminescence stability.

Acridinium dimethylphenyl ester labels are used in conjunction with magnetic microparticles in automated immunoassays in Siemens Healthcare Diagnostics' ADVIA Centaur® systems. Assay sensitivity is a function of both light output of the label and the background signal caused by non-specific binding of the label. While a large number of studies[19] have outlined how to devise protein-resistant surfaces either by PEG or zwitterion modification, similar studies on how to minimize non-specific binding of labels such as chemiluminescent acridinium esters are scant. In an earlier study,[1a] we reported that PEG introduction in the acridinium ring of alkoxy-substituted acridinium esters reduces their non-specific binding to paramagnetic microparticles (PMPs) and improves immunoassay performance. In the current study, we observed that the alkoxy-substituted acridinium ester **10a** with a more hydrophobic ring showed the maximum enhancement of light output in the presence of surfactants. To determine whether the polar sulfobetaine linker in the phenolic ester leaving group of this compound could counterbalance the hydrophobic acridinium ring, we measured the non-specific binding of anti-TSH antibody conjugate of this label as well as the conjugates of compounds **10c–10d** to PMPs. The conjugates were labeled to the same extent and contained 4–5 labels per antibody molecule.

The PMPs used for measurement of non-specific binding were, 1–10 micron-sized iron(III) oxide particles, coated with an anti-TSH antibody on the amino-silanized particle surface using commonly used glutaraldehyde coupling chemistry. The particles were mixed with solutions of the acridinium ester-labeled conjugates and were then magnetically separated, washed twice with water and then the chemiluminescence associated with the particles was measured. The ratio of this chemiluminescence value in comparison to the total chemiluminescence input is referred to asfractional non-specific binding (FNSB) and is a reflection of the resistance of the conjugate towards non-specific adsorption to the microparticles. The results of these measurements are tabulated in Table 6 and details are described in the Experimental section. The FNSB values in Table 6 indicate that the introduction of hydrophilic functional groups (sulfobetaine zwitterion or PEG) in the acridinium ring does not confer any additional advantage in the presence of a polar, zwitterionic linker in the phenolic ester leaving group. Conjugates of all four labels had similar values of non-specific binding with the conjugate of **10a** actually showing a two-fold decrease compared to **10d**. Thus, segregation of hydrophobic and hydrophilic structural features in the acridinium ring and phenolic ester respectively, appears to be an effective strategy in acridinium ester design for maximizing the impact of the surfactant on chemiluminescence without compromising non-specific binding.

Table 6 Non-specific binding of anti-TSH antibody conjugates of acridinium esters to PMPs[a]

Conjugate	FNSB[b]	Relative FNSB[c]
Anti-TSH-**10a**	7.3×10^{-5}	0.5
Anti-TSH-**10b**	1.3×10^{-4}	0.9
Anti-TSH-**10c**	2.2×10^{-4}	1.5
Anti-TSH-**10d**	1.5×10^{-4}	1.0[c]

[a] PMPs = paramagnetic particles. [b] FNSB = fractional non-specific binding. [c] Relative FNSB of label **10d** with an unsubstituted acridinium ring was assigned a value of one.

Conclusions

In the current study, we have investigated in detail for the first time how structural changes in the acridinium ring of chemiluminescent acridinium esters affect light emission in the presence of surfactants. Our results indicate that a relatively hydrophobic acridinium ring is needed to maximize the impact of the surfactant *i.e.* fast light emission and enhanced light output. The hydrophobicity of the acridinium ring can be offset by introducing a polar sulfobetaine linker in the phenolic ester leaving group so that non-specific binding of the label is not exacerbated. Among the three C-2 alkoxy-substituted acridinium esters that were synthesized in the current study, compound **10a** with a C-2 isopropyloxy group in the acridinium ring and a sulfobetaine linker in the phenolic ester, is likely to be a useful label for automated immunoassays. Not only does this compound exhibit fast emission and high light output (double that of **10d** with an unsubstituted acridinium ring), the label also exhibits good chemiluminescence stability and relatively low non-specific binding to magnetic microparticles. An added bonus is that this compound is the least bulky of the three alkoxy-substituted labels with a relatively straightforward synthesis.

Experimental

General

Chemicals and surfactants were purchased from Sigma-Aldrich (Milwaukee, Wisconsin, USA) unless indicated otherwise. Cetyltrimethylammonium chloride (CTAC) and hexa(ethylene)glycol monomethyl ether were purchased from TCI America. Cetyltripropylammonium chloride (CTPAC) was synthesized using a literature procedure.[20]

All final acridinium esters and intermediates were analyzed and/or purified by HPLC using a Beckman-Coulter HPLC system. TLC analysis was performed using 250 μm analytical silica plates from EM Separations Technologies. Flash chromatography was performed using glass columns or an 'Autoflash' system from ISCO. MALDI-TOF (matrix-assisted laser desorption ionization-time of flight) mass spectroscopy was performed using a Voyager DE™ Biospectrometry™ Workstation from Perkin-Elmer. This is a benchtop instrument operating in the linear mode with a 1.2 meter ion path length, flight tube. Spectra were acquired in positive ion mode. For small molecules, α-cyano-4-hydroxycinnamic acid was used as the matrix and spectra were acquired with an accelerating voltage of 20 000 volts and a delay time of 100 ns. For protein conjugates, sinapinic acid was used as the matrix and spectra were acquired with an accelerating voltage of 25 000 volts and a delay time of 85 ns.

For HRMS (high resolution mass spectra), samples were dissolved in HPLC-grade methanol and analyzed by direct-flow injection (injection volume = 5 μL) electrospray ionization (ESI) on a Waters Qtof API US instrument in the positive ion mode.

Optimized conditions were as follows: capillary = 3000 kV, cone = 35, source temperature = 120 °C, desolvation temperature = 350 °C. NMR spectra were recorded on a Varian 500 MHz spectrometer. IR spectra of neat samples were recorded on a Bruker TENSOR37 FT-IR spectrometer, ATR mode on ZnSe crystal. UV-Visible spectra were recorded on a Beckman DU 7500 spectrophotometer. Chemiluminescence measurements were carried out using a Berthold Technologies' AutoLumat Plus LB 953 luminometer.

1. Synthesis of acridinium esters (Fig. 3 and Fig. S1–S16 ESI†)

Compound 2. A solution of isatin (2.5 g, 0.017 mole) in anhydrous DMF (50 mL) was cooled in an ice bath under a nitrogen atmosphere and treated with sodium hydride (60% dispersion, 0.8 g, 1.5 equivalents). A purple solution was formed which was stirred at 0 °C for 30 min and then warmed to room temperature. A solution of 4-bromoanisole (2.13 mL, 0.017 mole) followed by copper(I) iodide (6.46 g, 0.034 mole) was added to this solution. The reaction was heated in an oil bath at 145 °C for 6–7 hours. It was then cooled to room temperature and diluted with an equal volume of ethyl acetate. The resulting suspension was filtered and the filtrate was concentrated under reduced pressure. TLC analysis using 25% ethyl acetate in hexanes showed clean formation of the *N*-arylated isatin with $R_f = 0.4$ (isatin $R_f = 0.25$).

The crude *N*-aryl isatin derivative (11.7 g) was refluxed in 10% KOH (150 mL) under a nitrogen atmosphere for 4 hours. It was then filtered while hot. The filtrate was diluted with water (150 mL) and ice. The resulting dark solution was then acidified with concentrated HCl until a yellow precipitate of compound **2** separated out. The acridine carboxylic acid **2** was recovered by filtration and dried under vacuum over P_2O_5 to give a yellowish-brown powder. Yield = 1.84 g (43%). TLC analysis showed a single spot of $R_f = 0.15$ using 25% methanol in chloroform as eluent. HPLC analysis of the product was performed using a Phenomenex, C_{18}, 10 micron, 3.9 × 300 mm column and a 40 min gradient of 10 → 40% MeCN–water (each with 0.05% TFA, TFA = trifluoroacetic acid) at a flow rate of 1.0 mL min^{-1} and UV detection at 260 nm. Product was observed eluting at 6.2 min. ν_{max}/cm^{-1} 3434 (OH), 1732 (CO), 1600, 1393, 1272, 1228. δ_H (500 MHz, CF_3COOD) 4.08 (s, 3H), 7.61 (br s, 1H), 7.99 (m, 1H), 8.01 (m, 1H), 8.23 (br t, 1H), 8.29 (br t, 2H), 8.41 (d, 1H, $J = 8.8$); MALDI-TOF MS *m/z* 253.9 $(M + H)^+$; HRMS *m/z* 254.0821 $(M + H)^+$ (254.0817 calculated).

Compound 3. A solution of 3,5-dimethyl-4-hydroxybenzoic acid (2 g, 0.012 mole) in methanol (50 mL) was cooled in an ice-bath under a nitrogen atmosphere. Thionyl chloride (5 mL) was added drop wise to the cold methanol solution. After completion of the addition, the reaction was warmed to room temperature and stirred for 48 hours. The reaction was then neutralized with the addition of solid sodium bicarbonate until gas evolution ceased. The suspension was evaporated to dryness. The residue was partitioned between ethyl acetate (100 mL) and de-ionized water (50 mL). The ethyl acetate layer was washed with brine, dried over anhydrous magnesium sulfate and concentrated under reduced pressure to give a tan powder. TLC analysis of the product using 2% ethyl acetate in chloroform showed a single spot of $R_f = 0.4$. HPLC analysis of the product was performed using a Phenomenex, C_{18}, 10 micron, 3.9 × 300 mm column and a 40 min gradient of 10 → 60% MeCN–water (each with 0.05% TFA) at a flow rate of 1.0 mL min^{-1} and UV detection at 260 nm. Product was observed eluting at 20 min. Yield = 1.98 g (91%). ν_{max}/cm^{-1} 3347 (OH), 1686 (CO), 1599, 1435, 1320, 1277, 1183.

δ_H (500 MHz, $CDCl_3$) 2.27 (s, 6H), 3.87 (s, 3H), 7.70 (s, 2H); MALDI-TOF MS *m/z* 180.9 $(M + H)^+$; HRMS *m/z* 181.0873 $(M + H)^+$ (181.0865 calculated).

Compound 4. Compound **3** (1.506 g, 8.36 mmoles) and *p*-toluenesulfonyl chloride (2.390 g, 12.54 mmoles) were added to a suspension of compound **2** (2.54 g, 10.03 mmoles) in anhydrous pyridine (80 mL). The reaction was stirred at room temperature for 4 hours under a nitrogen atmosphere. The reaction mixture was then concentrated by rotary evaporation. The residue was extracted with dichloromethane (80 mL) and washed with cold 1 N HCl (10 mL), brine (20 mL × 2), cold 1% NaOH (20 mL) and brine (20 mL × 2) in that order. The organic layer was dried over anhydrous magnesium sulfate, filtered and concentrated by rotary evaporation. The product was purified by flash chromatography on silica using 20% ethyl acetate in hexanes as eluent. Yield = 3.0 g (86%, yellow powder). TLC analysis using 40% ethyl acetate in hexanes showed a single spot of $R_f = 0.63$. HPLC analysis of the purified product was performed using a Phenomenex, C_{18}, 10 micron, 3.9 × 300 mm column and a 30 min gradient of 10 → 100% MeCN–water (each with 0.05% TFA) at a flow rate of 1.0 mL min^{-1} and UV detection at 260 nm. Product was observed eluting at 23 min. ν_{max}/cm^{-1} 1739 and 1720 (CO), 1632, 1611, 1473, 1434, 1323, 1226, 1149. δ_H (500 MHz, $CDCl_3$) 2.49 (s, 6H), 3.95 (s, 3H), 3.97 (s, 3H), 7.57 (dd, 1H, $J = 9.4, 2.7$), 7.58 (d, $J = 2.7$), 7.67 (m, 1H), 7.79 (m, 1H), 7.92 (s, 2H), 8.21 (d, 1H, $J = 9.4$), 8.30 (d, 1H, $J = 8.2$), 8.42 (d, 1H, $J = 8.5$); MALDI-TOF MS *m/z* 416.6 $(M + H)^+$; HRMS *m/z* 416.1497 $(M + H)^+$ (416.1498 calculated).

Compound 5. A solution of boron tribromide in dichloromethane (1.0 M, 40 mL, 40.0 mmoles) was added to a solution of compound **4** (2.84 g, 6.84 mmoles) in dichloromethane (40 mL). The reaction was stirred at room temperature for 4 hours. The reaction mixture was cooled to 0 °C and MeOH (200 mL) added slowly. The reaction mixture was allowed to gradually warm to room temperature and was stirred for 16 hours. The reaction mixture was then cooled again to 0 °C and solid sodium bicarbonate was added in portions until gas evolution ceased. The reaction mixture was then concentrated by rotary evaporation. The residue was partitioned between ethyl acetate (150 mL) and de-ionized water (50 mL). The organic layer was separated and washed with brine (50 mL). It was then dried over anhydrous magnesium sulfate, filtered and concentrated under reduced pressure. The product was purified by flash chromatography on silica (ISCO Autoflash system) using a 20 min gradient of 0 → 50% ethyl acetate in hexanes as eluent at a flow rate of 40 mL min^{-1} and UV detection at 260 nm. Concentration of the product fractions afforded an orange-yellow solid. Yield = 2.46 g (90%). TLC analysis using 20% ethyl acetate in hexanes showed a single spot of $R_f = 0.14$. HPLC

analysis of the purified product was performed using a Phenomenex, C_{18}, 10 micron, 3.9 × 300 mm column and a 30 min gradient of 10 → 70% MeCN–water (each with 0.05% TFA) at a flow rate of 1.0 mL min^{-1} and UV detection at 260 nm. Product was observed eluting at 25.5 min. ν_{max}/cm^{-1} 1746 and 1718 (CO), 1631, 1609, 1460, 1323, 1231, 1137. δ_H (500 MHz, $CDCl_3$) 2.30 (s, 6H), 3.91 (s, 3H), 7.54 (dd, 1H, J = 9.3, 2.6), 7.63 (m, 1H), 7.70 (d, 1H, J = 2.4), 7.76 (m, 1H), 7.81 (s, 2H), 8.27 (d, 1H, J = 9.4), 8.31 (d, 1H, J = 8.8), 8.38 (d, 1H, J = 8.8); MALDI-TOF MS m/z 401.1 $(M + H)^+$; HRMS m/z 402.1334 $(M + H)^+$ (402.1341 calculated).

Compound 6a. A solution of compound **5** (0.25 g, 0.62 mmole), triphenylphosphine (0.327 g, 1.25 mmoles) and 2-propanol (0.096 mL, 1.13 mmoles) in anhydrous tetrahydrofuran (10 mL) at 0 °C was treated with diisopropyl azodicarboxylate (DIAD, 0.244 mL, 1.24 mmoles) under a nitrogen atmosphere. The reaction was stirred at 0 °C for one hour by which time TLC analysis using 20% ethyl acetate in hexanes showed complete conversion to a less polar product of R_f = 0.4 (starting material R_f = 0.14). The reaction was concentrated by rotary evaporation to ~5 mL and the product was purified by flash chromatography on silica using 10% ethyl acetate in hexanes as eluent. HPLC analysis of the purified product was performed using a Phenomenex, C_{18}, 10 micron, 3.9 × 300 mm column and a 30 min gradient of 10 → 100% MeCN–water (each with 0.05% TFA) at a flow rate of 1.0 mL min^{-1} and UV detection at 260 nm. Product was observed eluting at 30 min. Yield = 0.26 g (93%, yellow sticky solid). ν_{max}/cm^{-1} 1743 and 1716 (CO), 1633, 1612, 1466, 1323, 1228, 1210, 1132. δ_H (500 MHz, $CDCl_3$) 1.44 (d, 6H, J = 6.1), 2.47 (s, 6H), 3.95 (s, 3H), 4.74 (spt, 1H, J = 6.1), 7.52 (m, 1H), 7.58 (d, 1H, J = 2.8), 7.67 (m, 1H), 7.80 (m, 1H), 7.92 (s, 2H), 8.27 (br s, 1H), 8.34 (br s, 1H), 8.43 (d, 1H, J = 8.2); MALDI-TOF MS m/z 445.8 $(M + H)^+$; HRMS m/z 444.1805 $(M + H)^+$ (444.1811 calculated).

Compound 6b. A solution of compound **5** (0.025 g, 0.062 mmole), triphenylphosphine (0.033 g, 0.13 mmole) and 3-dimethylamino-1-propanol (0.015 mL, 0.13 mmole) in anhydrous tetrahydrofuran (3 mL) at room temperature was treated with DIAD (0.025 mL, 0.124 mmole) under a nitrogen atmosphere. The reaction was stirred for one hour by which time TLC analysis using 1 : 1, methanol–ethyl acetate showed complete conversion to a polar product of R_f = 0.2. Using ethyl acetate as eluent, starting material was completely consumed. The reaction was diluted with ethyl acetate (25 mL) and 1 N HCl (25 mL). The HCl layer was separated and washed with ethyl acetate (2 × 25 mL). It was then cooled in ice and treated with 5% KOH until the product precipitated out. The resulting suspension was extracted twice with ethyl acetate (2 × 25 mL). The combined ethyl acetate extracts were dried over anhydrous magnesium sulfate, filtered and concentrated under reduced pressure to afford a yellow solid. HPLC analysis of the product was performed using a Phenomenex, C_{18}, 10 micron, 3.9 × 300 mm column and a 30 min gradient of 10 → 70% MeCN–water (each with 0.05% TFA) at a flow rate of 1.0 mL min^{-1} and UV detection at 260 nm. Product was observed eluting at 25 min. Yield = 24.5 mg (80%). ν_{max}/cm^{-1} 1741 and 1715 (CO), 1631, 1611, 1442, 1321, 1225, 1146, 1128. δ_H (500 MHz, $CDCl_3$) 2.20 (m, 2H), 2.47 (s, 12H), 2.74 (m, 2H), 3.94 (s, 3H), 4.18 (t, 2H, J = 6.1), 7.52 (dd, 1H, J = 9.3, 2.6), 7.56 (d, 1H, J = 2.5), 7.66 (m, 1H), 7.79 (m, 1H), 7.92 (s, 2H), 8.20 (d, 1H, J = 9.4), 8.29 (d, 1H, J = 8.2), 8.41 (d, 1H, J = 8.2); MALDI-TOF MS m/z 487.5 $(M + H)^+$; HRMS m/z 487.2228 $(M + H)^+$ (487.2233 calculated).

Compound 6c. A solution of compound **5** (0.05 g, 0.125 mmole), triphenylphosphine (0.065 g, 0.25 mmole) and hexa(ethylene)glycol monomethyl ether (0.055 g, 0.186 mmole) in anhydrous tetrahydrofuran (5 mL) was treated with DIAD (0.05 mL, 0.25 mmole) under a nitrogen atmosphere. The reaction was stirred at room temperature for one hour by which time TLC analysis using 5% methanol in ethyl acetate showed complete conversion to a polar product of R_f = 0.5. No starting material was present when the reaction was analyzed by TLC using 1 : 1 ethyl acetate–hexanes. The product was purified by flash chromatography on silica using 2% methanol in ethyl acetate as eluent. HPLC analysis of the purified product was performed using a Phenomenex, C_{18}, 10 micron, 3.9 × 300 mm column and a 30 min gradient of 10 → 70% MeCN–water (each with 0.05% TFA) at a flow rate of 1.0 mL min^{-1} and UV detection at 260 nm. Product was observed eluting at 29 min. Yield = 0.032 g (38%, yellow sticky solid). ν_{max}/cm^{-1} 1747 and 1712 (CO), 1631, 1447, 1323, 1235, 1181, 1130, 1097. δ_H (500 MHz, $CDCl_3$) 2.47 (s, 6H), 3.36 (s, 3H), 3.53 (m, 2H), 3.61–3.63 (m, 2H), 3.64 (br s, 12H), 3.69 (m, 2H), 3.75 (m, 2H), 3.95 (s, 3H), 3.96–3.98 (m, 2H), 4.30 (br t, 2H), 7.61 (d, 1H, J = 2.4), 7.86–7.91 (m, 2H), 7.93 (s, 2H), 8.09 (m, 1H), 8.49 (d, 1H, J = 8.9), 8.85 (m, 2H); MALDI-TOF MS m/z 679.7 $(M + H)^+$; HRMS m/z 680.3070 $(M + H)^+$ (680.3071 calculated).

Compound 7a. A mixture of compound **6a** (0.213 g, 0.48 mmole), 1,3-propane sultone (0.88 g, 7.2 mmoles, 15 equivalents) and 2,6-di-*tert*-butylpyridine (0.79 mL, 3.5 mmoles) in 1-butyl-3-methylimidazolium hexafluorophosphate [BMIM][PF_6] (3 mL) was heated at 155 °C in a round bottom flask under argon with vigorous stirring. After 16 hours, the reaction was cooled to room temperature. A small portion of the reaction (0.002 mL) was withdrawn, diluted with MeCN (0.1 mL) and analyzed by HPLC using a Phenomenex, C_{18}, 10 micron, 3.9 × 300 mm column and a 30 min gradient of 10 → 100% MeCN–water (each with 0.05% TFA) at a flow rate of 1.0 mL min^{-1} and UV detection at 260 nm. The *N*-sulfopropyl acridinium ester (methyl ester of compound **7a**) was observed eluting at 19.5 min (90% conversion). The reaction was diluted with ethyl acetate (5 mL) and loaded onto a silica column equilibrated with ethyl acetate. The column was eluted with ethyl acetate (500 mL) to elute unreacted starting material and base followed by 40% methanol in ethyl acetate to elute product. The fractions containing the acridinium ester were concentrated under reduced pressure. The *N*-sulfopropyl acridinium ester (0.25 g) was refluxed in 20 mL of 2 N HCl for 3 hours. It was then cooled to room temperature. HPLC analysis as described above showed complete conversion to compound **7a** eluting at 15.5 min. The reaction mixture was concentrated by rotary evaporation to ~10 mL and diluted with MeCN (10 mL). The product **7a** was purified by preparative HPLC using a YMC, C_{18}, 10 micron, 30 × 250 mm column and 30 min gradient of 10

→ 100% MeCN–water (each with 0.05% TFA) at a solvent flow rate of 20 mL min^{-1} and UV detection at 260 nm. The HPLC fractions containing product **7a** were combined and concentrated under reduced pressure to give a yellow, sticky solid. Yield = 0.12 g (45%). TLC analysis (1 : 4, MeOH–ethyl acetate with a drop of acetic acid) showed product with R_f = 0.4. ν_{max}/cm^{-1} 3477 and 3415 (OH), 1743 and 1705 (CO), 1633, 1556, 1465, 1385, 1307, 1148 1097. δ_H (500 MHz, CF_3COOD) 1.48 (d, 6H, J = 6.1), 2.53 (s, 6H), 2.89 (m, 2H), 3.78 (t, 2H, J = 6.0), 4.88 (spt, 1H, J = 6.0), 5.79 (m, 2H), 7.83 (d, 1H, J = 2.4), 8.04 (m, 3H), 8.16 (m, 1H), 8.38 (m, 1H), 8.67 (d, 1H, J = 8.6), 8.80 (m, 2H); MALDI-TOF MS m/z 553.2 $(M + H)^+$; HRMS m/z 552.1688 $(M + H)^+$ (552.1692 calculated).

Compound 7b. A mixture of compound **6b** (0.025 g, 0.050 mmole), 1,3-propane sultone (0.125 g, 1.02 mmoles, 20 equivalents) and 2,6-di-*tert*-butylpyridine (0.079 mL, 0.35 mmole) in [BMIM]PF_6] (0.5 mL) was heated at 150 °C under argon for 24 hours. It was then cooled to room temperature and analyzed by HPLC using a Phenomenex, C_{18}, 10 micron, 3.9 × 300 mm column and a 30 min gradient of 10 → 70% MeCN–water (each with 0.05% TFA) at a flow rate of 1.0 mL min^{-1} and UV detection at 260 nm. The di-alkylated product (methyl ester of compound **7b**) was observed eluting at 18 min (>80% conversion). The crude reaction mixture was partitioned between water and ethyl acetate (25 mL each). The aqueous layer containing product was separated and washed once with ethyl acetate (50 mL). It was then concentrated under reduced pressure. The residue was refluxed in 1 N HCl (10 mL) for 2 hours under a nitrogen atmosphere. The reaction was cooled to room temperature and analyzed by HPLC as described above which showed complete conversion to compound **7b** eluting at 14.3 min. The product **7b** was purified by preparative HPLC using a YMC, C_{18}, 10 micron, 30 × 250 mm column and 30 min gradient of 10 → 70% MeCN–water (each with 0.05% TFA) at a solvent flow rate of 20 mL min^{-1} and UV detection at 260 nm. The HPLC fractions containing product **7b** were combined and concentrated under reduced pressure to give a yellow, sticky solid. Yield = 0.032 g (88%). TLC analysis (2 : 1, MeOH–ethyl acetate with a drop of acetic acid) showed product with R_f = 0.17. ν_{max}/cm^{-1} 3421 (OH), 1750 and 1702 (CO), 1630, 1555, 1468, 1378, 1307, 1186, 1147, 1035. δ_H (500 MHz, CF_3COOD) 2.51 (s, 6H), 2.55 (m, 4H), 2.88 (m, 2H), 3.24 (s, 6H), 3.42 (t, 2H, J = 5.7), 3.70–3.80 (m, 6H), 4.38 (br s, 2H), 5.82 (m, 2H), 7.82 (br s, 1H), 8.04 (s, 2H), 8.08 (m, 1H), 8.17 (br d, 1H), 8.43 (m, 1H), 8.75 (br d, 1H), 8.83 (d, 1H, J = 9.2), 8.89 (d, 1H, J = 9.5); MALDI-TOF MS m/z 717.1 $(M + H)^+$; HRMS m/z 717.2161 $(M + H)^+$ (717.2152 calculated).

Compound 7c. A mixture of compound **6c** (0.295 g, 0.434 mmole), 1,3-propane sultone (0.795 g, 6.51 mmoles) and 2,6-di-*tert*-butylpyridine (0.72 mL, 3.25 mmoles) in [BMIM][PF_6] (2.6 mL) was heated at 150 °C under argon. After 24 hours, the reaction was cooled to room temperature and analyzed by HPLC using a Phenomenex, C_{18}, 10 micron, 3.9 × 300 mm column and a 30 mine gradient of 10 → 70% MeCN–water (each with 0.05% TFA) at a flow rate of 1.0 mL min^{-1} and UV detection at 260 nm. The *N*-sulfopropyl acridinium ester (methyl ester of compound **7c**) was observed eluting at 21.5 min. The reaction was diluted with ethyl acetate and purified by flash chromatography as described previously for compound **7a**. Yield = 0.187 g (54%). The acridinium methyl ester (120 mg) was refluxed in 1 N HCl (5 mL) for 1.5 hours. It was then cooled to room temperature and analyzed by HPLC which showed complete conversion to compound **7c** eluting at 18.5 min. The product was purified by preparative HPLC using a YMC, C_{18}, 10 micron, 30 × 250 mm column and 30 min gradient of 10 → 70% MeCN–water (each with 0.05% TFA) at a solvent flow rate of 20 mL min^{-1} and UV detection at 260 nm. The HPLC fractions containing product **7c** were combined and concentrated under reduced pressure to give a yellow, sticky solid. Yield = 78 mg (66% from acridinium methyl ester). TLC analysis (2 : 1, MeOH–ethyl acetate with a drop of acetic acid) showed product with R_f = 0.40. ν_{max}/cm^{-1} 3420 (OH), 1750 and 1709 (CO), 1628, 1554, 1473, 1448, 1379, 1305, 1143, 1102, 1034. δ_H (500 MHz, CF_3COOD) 2.52 (s, 6H), 2.88 (m, 2H), 3.53 (s, 3H), 3.78 (t, 2H, J = 6.0), 3.87–3.89 (br s, 14H), 3.91–3.94 (m, 2H), 4.01–4.07 (m, 2H), 4.20 (br s, 2H), 4.47 (br s, 2H), 5.81 (br s, 2H), 7.82 (br s, 1H), 8.03 (s, 2H), 8.06 (m, 1H), 8.17 (m, 1H), 8.41 (m, 1H), 8.71 (d, 1H, J = 8.7), 8.84 (m, 2H); MALDI-TOF MS m/z 787.9 $(M + H)^+$; HRMS m/z 788.2950 $(M + H)^+$ (788.2952 calculated).

Compound 9a. A solution of compound **7a** (0.120 g, 0.217 mmole) in DMF (4 mL) was treated with diisopropylethylamine (0.076 mL, 0.44 mmole) and *N*,*N*,*N*′,*N*′-tetramethyl-*O*-(*N*-succinimidyl)uronium tetrafluoroborate (TSTU) (0.079 g, 0.26 mmole). The reaction was stirred at room temperature. After 15 min the reaction was analyzed by HPLC using a Phenomenex, C_{18}, 10 micron, 3.9 × 300 mm column and a 30 min gradient of 10 → 100% MeCN–water (each with 0.05% TFA) at a flow rate of 1.0 mL min^{-1} and UV detection at 260 nm. The NHS ester of compound **9a** was observed eluting at 18.5 min. This solution was added drop wise to a chilled solution of compound **8** (0.4 g, 0.89 mmole, HBr salt) dissolved in a mixture of 0.25 M sodium bicarbonate (8 mL) and DMF (2 mL). The resulting reaction was stirred at room temperature. After 30 min, HPLC analysis indicated complete conversion to compound **9a** eluting at 12 min. Using a gradient of 10 → 70% MeCN–water (each with 0.05% TFA), product eluted at 14 min. The product was purified by preparative HPLC using a YMC, C_{18}, 10 micron, 30 × 250 mm column and 30 min gradient of 10 → 100% MeCN–water (each with 0.05% TFA) at a solvent flow rate of 20 mL min^{-1} and UV detection at 260 nm. The HPLC fractions containing product **9a** were combined and concentrated under reduced pressure to give a yellow, sticky solid. Yield = 0.13 g (65%, TFA salt). ν_{max}/cm^{-1} 3416 (NH), 1750 and 1706 (CO), 1630, 1554, and 1468, 1378, 1307, 1186, 1147, 1035. δ_H (500 MHz, CF_3COOD) 1.49 (d, 6H, J = 6.0), 2.36 (m, 2H), 2.52 (s, 10H), 2.89 (m, 2H), 3.20 (s, 3H), 3.42 (m, 4H), 3.61 (m, 4H), 3.77 (br m, 6H), 4.87 (m, 1H), 5.79 (br t, 2H), 7.67 (s, 2H), 7.79 (s, 1H), 8.04 (br t, 1H), 8.17 (br d, 1H), 8.39 (br t, 1H), 8.64 (d, 1H, J = 8.7), 8.80 (br d, 2H); MALDI-TOF MS m/z 802.7 $(M + H)^+$; HRMS m/z 823.3028 $(M + Na)^+$ (823.3023 calculated).

Compound 9b. A solution of compound **7b** (0.032 g, 0.045 mmole) in DMF (3.4 mL) and de-ionized water (0.6 mL) was treated with diisopropylethylamine (0.039 mL, 0.22 mmole)

and TSTU (0.067 g, 0.22 mmole). The reaction was stirred at room temperature. After 15 min, the reaction was analyzed by HPLC using a Phenomenex, C_{18}, 10 micron, 3.9 × 300 mm column and a 30 min gradient of 10 → 70% MeCN–water (each with 0.05% TFA) at a flow rate of 1.0 mL min^{-1} and UV detection at 260 nm. The NHS ester of compound **9b** was observed eluting at 17 min. The NHS ester was purified by preparative HPLC using a YMC, C_{18}, 10 micron, 30 × 250 mm column and 30 min gradient of 10 → 70% MeCN–water (each with 0.05% TFA) at a solvent flow rate of 20 mL min^{-1} and UV detection at 260 nm. The HPLC fractions containing the NHS ester were frozen at −80 °C and lyophilized to afford a yellow powder. Yield = 25 mg (69%). A solution of this NHS ester (0.01 g, 0.012 mmole) in DMSO (1 mL) was added drop wise to a chilled solution of compound **8** (0.027 g, 0.06 mmole, HBr salt) dissolved in 0.25 M sodium bicarbonate (0.6 mL). The resulting solution was stirred at room temperature. After 30 minutes the reaction was analyzed by HPLC using a Phenomenex, C_{18}, 10 micron, 3.9 × 300 mm column and a 30 min gradient of 10 → 70% MeCN–water (each with 0.05% TFA) at a flow rate of 1.0 mL min^{-1} and UV detection at 260 nm. Product **9b** was observed eluting at 13.5 min. The product was purified by preparative HPLC using a YMC, C_{18}, 10 micron, 30 × 250 mm column and 30 min gradient of 10 → 70% MeCN–water (each with 0.05% TFA) at a solvent flow rate of 20 mL min^{-1} and UV detection at 260 nm. The HPLC fractions containing **9b** were concentrated under reduced pressure. Yield = 8.5 mg (71%). ν_{max}/cm^{-1} 3408 (NH), 1745 and 1670 (CO), 1629, 1554, 1467, 1377, 1159, 1036. δ_H (500 MHz, CF_3COOD) 2.38 (br s, 2H), 2.54 (s, 6H), 2.57 (m, 4H), 2.92 (m, 2H), 3.24 (s, 3H), 3.29 (s, 6H), 3.41 (br s, 6H), 3.47 (br s, 4H), 3.65 (br s, 4H), 3.70–3.90 (br m, 10H), 4.42 (br s, 2H), 5.82 (m, 2H), 7.17 (br s, 1H), 7.72 (br s, 2H), 7.83 (br s, 1H), 8.13 (m, 1H), 8.22 (d, 1H, J = 9.8), 8.48 (m, 1H), 8.78 (d, 1H, J = 8.6), 8.85 (d, 1H, J = 9.8), 8.92 (d, 1H, J = 10.0); MALDI-TOF MS m/z 965.5 $(M + H)^+$; HRMS m/z 966.3660 $(M + H)^+$ (966.3663 calculated).

Compound 9c. A solution of compound **7c** (0.0082 g, 0.01 mmole) in DMF (1.5 mL) was treated with diisopropylethylamine (0.0036 mL, 0.02 mmole) and TSTU (0.0047 g, 0.016 mmole). The reaction was stirred at room temperature. After 15 min, the reaction was analyzed by HPLC using a Phenomenex, C_{18}, 10 micron, 3.9 × 300 mm column and a 30 min gradient of 10 → 70% MeCN–water (each with 0.05% TFA) at a flow rate of 1.0 mL min^{-1} and UV detection at 260 nm. The NHS ester of compound **9c** was observed eluting at 20.5 min. This solution was added drop wise to a chilled solution of compound **8** (0.035 g, 0.078 mmole, HBr salt) dissolved in DMSO (0.28 mL) and 0.25 M sodium bicarbonate (0.6 mL). The resulting solution was stirred at room temperature. After 30 min, HPLC analysis indicated complete conversion to compound **9c** eluting at 13.5 min. The product was purified by preparative HPLC using a YMC, C_{18}, 10 micron, 30 × 250 mm column and 30 min gradient of 10 → 70% MeCN–water (each with 0.05% TFA) at a solvent flow rate of 20 mL min^{-1} and UV detection at 260 nm. The HPLC fractions containing **9c** were concentrated under reduced pressure. Yield = 11.2 mg (85%, TFA salt). ν_{max}/cm^{-1} 3396 (NH), 1747 and 1677 (CO), 1630, 1553 and 1474, 1195, 1161, 1125, 1038. δ_H (500 MHz, CF_3COOD) 2.38 (m, 2H), 2.54 (s, 6H), 2.91 (m, 2H), 3.22 (m, 3H), 3.32–3.50 (m, 4H), 3.56 (s, 3H), 3.63 (m, 4H), 3.69–3.83 (m, 6H), 3.85 (m, 2H), 3.88–3.96 (br s, 14H), 3.97 (m, 2H), 4.08 (m, 2H), 4.23 (br s, 2H), 4.49 (br s, 2H), 5.83 (m, 2H), 7.69 (s, 2H), 7.83 (d, 1H, J = 2.1), 8.03 (s, 2H), 8.10 (m, 1H), 8.21 (dd, 1H, J = 9.9, 2.0), 8.45 (m, 1H), 8.72 (d, 1H, J = 8.9), 8.86 (m, 2H); MALDI-TOF MS m/z 1036.4 $(M + H)^+$; HRMS m/z 1037.4460 $(M + H)^+$ (1037.4463 calculated).

Compound 10a. A solution of compound **9a** (0.05 g, 0.053 mmole, TFA salt) in 1 : 1 DMF–methanol (5 mL) was treated with diisopropylethylamine (0.054 mL, 0.31 mmole) and glutaric anhydride (0.036 g, 0.32 mmole). The reaction was stirred at room temperature. After one hour the reaction was analyzed by HPLC using a Phenomenex, C_{18}, 10 micron, 3.9 × 300 mm column and a 30 min gradient of 10 → 70% MeCN–water (each with 0.05% TFA) at a flow rate of 1.0 mL min^{-1} and UV detection at 260 nm. The glutarate derivative of compound **9a** was observed eluting at 16 min (complete conversion). The reaction was diluted with toluene (5 mL) and concentrated under reduced pressure. The crude glutarate derivative was dissolved in DMF (6 mL) and treated with diisopropylethylamine (0.109 mL, 0.63 mmole) and TSTU (0.187 g, 0.62 mmole). The reaction was stirred at room temperature. After 30 min the reaction was analyzed by HPLC which indicated >80% conversion to **10a** eluting at 17 min. The NHS ester was purified by preparative HPLC using a YMC, C_{18}, 10 micron, 30 × 250 mm column and 30 min gradient of 10 → 70% MeCN–water (each with 0.05% TFA) at a solvent flow rate of 20 mL min^{-1} and UV detection at 260 nm. The HPLC fractions containing the NHS ester were frozen at −80 °C and lyophilized to afford a yellow powder. Yield = 61 mg (quantitative). ν_{max}/cm^{-1} 3290 (NH), 1815, 1782 and 1733 and 1653 (CO), 1553, 1449, 1375, 1199, 1157, 1069, 1037. δ_H (500 MHz, CF_3COOD) 1.49 (d, 6H, J = 6.0), 2.36 (m, 2H), 2.52 (s, 10H), 2.89 (m, 2H), 3.20 (s, 3H), 3.42 (m, 4H), 3.61 (m, 4H), 3.77 (br m, 6H), 4.87 (m, 1H), 5.79 (br t, 2H), 7.67 (s, 2H), 7.79 (s, 1H), 8.04 (br t, 1H), 8.17 (br d, 1H), 8.39 (br t, 1H), 8.64 (d, 1H, J = 8.7), 8.80 (br d, 2H); MALDI-TOF MS m/z 1014.2 $(M + H)^+$; HRMS m/z 1034.3501 $(M + Na)^+$ (1034.3503 calculated).

Compound 10b. A solution of compound **9b** (8.5 mg, 0.008 mmole) in 10% aqueous methanol (3.5 mL) was treated with diisopropylethylamine (0.0077 mL, 0.044 mmole) and glutaric anhydride (4.5 mg, 0.04 mmole). The reaction was stirred at room temperature. After 15 min the reaction was analyzed by HPLC using a Phenomenex, C_{18}, 10 micron, 3.9 × 300 mm column and a 30 min gradient of 10 → 100% MeCN–water (each with 0.05% TFA) at a flow rate of 1.0 mL min^{-1} and UV detection at 260 nm. The glutarate derivative of compound **9b** was observed eluting at 12 min (~90% conversion). The reaction was diluted with toluene (2 mL) and concentrated under reduced pressure. The glutarate derivative was dissolved in 10% aqueous DMF (3 mL) and treated with diisopropylethylamine (0.0154 mL, 0.088 mmole) and TSTU (26.4 mg, 0.088 mmole). The reaction was stirred at room temperature. After 10 min, HPLC analysis indicated complete conversion to **10b** eluting at 13 min. The NHS ester was purified by preparative HPLC using a YMC, C_{18}, 10 micron, 30 × 250 mm column and 30 min

gradient of 10 → 70% MeCN–water (each with 0.05% TFA) at a solvent flow rate of 20 mL min^{-1} and UV detection at 260 nm. The HPLC fractions containing the NHS ester were frozen at −80 °C and lyophilized to afford a yellow powder. Yield = 7.5 mg (73%). ν_{max}/cm^{-1} 3290 (NH), 1809, 1782, 1734 and 1674 (CO), 1557, 1467, 1442, 1379, 1196, 1160, 1131, 1036. δ_H (500 MHz, CF_3COOD) 2.10–2.39 (m, 6H), 2.39–2.71 (m, 10H), 2.78 (br s, 4H), 2.90 (m, 4H), 3.03 (s, 3H), 3.09–3.35 (m, 12H), 3.40 (m, 4H), 3.56 (m, 4H), 3.65–3.99 (m, 12H), 4.41 (br s, 2H), 5.84 (br s, 2H), 7.72 (br s, 2H), 7.81 (br s, 1H), 8.09 (br t, 1H), 8.18 (d, 1 H, J = 9.2), 8.44 (br t, 1H), 8.74 (d, 1H, J = 8.5), 8.84 (d, 1H, J = 10), 8.91 (d, 1H, J = 8.5); MALDI-TOF MS m/z 1179.1 $(M + H)^+$; HRMS m/z 1177.4152 $(M + H)^+$ (1177.4144 calculated).

Compound 10c. A solution of compound **9c** (11.2 mg, 0.01 mmole) in methanol (1 mL) was treated with diisopropylethylamine (0.0086 mL, 0.049 mmole) and glutaric anhydride (5.6 mg, 0.049 mmole). The reaction was stirred at room temperature. After 15 min the reaction was analyzed by HPLC using a Phenomenex, C_{18}, 10 micron, 3.9 × 300 mm column and a 30 min gradient of 10 → 70% MeCN–water (each with 0.05% TFA) at a flow rate of 1.0 mL min^{-1} and UV detection at 260 nm. The glutarate derivative of compound **9c** was observed eluting at 15.4 min. The glutarate derivative was purified by preparative HPLC using a YMC, C_{18}, 10 micron, 30 × 250 mm column and 30 min gradient of 10 → 70% MeCN–water (each with 0.05% TFA) at a solvent flow rate of 20 mL min^{-1} and UV detection at 260 nm. The product fraction was concentrated under reduced pressure. The glutarate (9 mg, 0.0072 mmole) was dissolved in DMF (1 mL) and treated with diisopropylethylamine (0.0063 mL, 0.036 mmole) and TSTU (10.8 mg, 0.036 mmole). The reaction was stirred at room temperature. After 15 min, HPLC analysis indicated 80% conversion to compound **10c** eluting at 16.5 min. The NHS ester was purified by preparative HPLC using a YMC, C_{18}, 10 micron, 30 × 250 mm column and 30 min gradient of 10 → 70% MeCN–water (each with 0.05% TFA) at a solvent flow rate of 20 mL min^{-1} and UV detection at 260 nm. The HPLC fractions containing the NHS ester were frozen at −80 °C and lyophilized to afford a yellow, sticky solid. Yield = 5 mg (57%). ν_{max}/cm^{-1} 3216 (NH), 1815, 1782 and 1725 (CO), 1430, 1362, 1200, 1070, 1049. δ_H (500 MHz, CF_3COOD) 2.06–2.40 (m, 6H), 2.54 (br s, 6H), 2.62 (br s, 2H), 2.78 (br s, 2H), 2.85–2.97 (m, 4H), 3.04 (br s, 4H), 3.17 (br s, 4H), 3.31 (m, 6H), 3.41 (br s, 4H), 3.55 (s, 6H), 3.79 (m, 6H), 3.85 (br s, 2H), 3.89 (br s, 10H), 3.96 (br s, 2H), 4.07 (br s, 2H), 4.22 (br s, 2H), 4.48 (br s, 2H), 5.82 (br s, 2H), 7.71 (br s, 2H), 7.82 (br s, 2H), 8.08 (br t, 1H), 8.19 (d, 1H, J = 9.6), 8.44 (br t, 1H), 8.70 (br d, 1H), 8.85 (br t, 2H); MALDI-TOF MS m/z 1247.5 $(M + H)^+$; HRMS m/z 1270.4802 $(M + Na)^+$ (1270.4773 calculated).

2. Synthesis of anti-TSH antibody conjugates

A murine anti-TSH monoclonal antibody with an acidic pI = 5.6 (TSH = thyroid stimulating hormone) was used for labeling with the acridinium ester labels **10a–10c**.

The anti-TSH murine monoclonal antibody (1 mg, 6.67 nanomoles, stock solution 5 mg mL^{-1}, 0.2 mL) was diluted with 0.2 mL of 0.1 M sodium carbonate, pH 9. The protein solution was treated with DMSO solutions of acridinium esters **10a–10c** as follows: for labeling with 7.5 equivalents of **10a**, 0.0051 mL of a 10 mg mL^{-1} DMSO was added; for labeling with 10 equivalents of **10b**, 0.0157 mL of a 5 mg mL^{-1} DMSO solution was added; and, for labeling with 10 equivalents of **10c**, 0.0166 mL of a 5 mg mL^{-1} DMSO solution was added. The labeling reactions were stirred at 4 °C for 16 hours and were then transferred to 4 mL Amicon™ filters (MW 30 000 cutoff) and diluted with 3.5 mL de-ionized water. The volume was reduced to ~0.1 mL by centrifuging at 4000 G for 10 min. The concentrated conjugate solutions were diluted with 4 mL de-ionized water and centrifuged again to reduce the volume. This process was repeated a total of four times. Finally, the concentrated conjugates were diluted with 0.1 mL de-ionized water. The conjugates were analyzed by MALDI-TOF mass spectrometry, using the Voyager-DE instrument from Perkin-Elmer, to measure acridinium ester incorporation. This entailed measuring the molecular weight of the unlabeled protein and the labeled protein. The acridinium ester label contributed to the observed difference in mass between these two measurements. By knowing the molecular weight of the specific acridinium ester label, the extent of label incorporation for that specific acridinium ester could thus be calculated. Label incorporation in each protein is given in Table 7.

3. Emission wavelength measurements (Fig. 4)

Visible wavelength emission spectra of the acridinium esters **10a–10d** were measured using a FSSS (Fast Spectral Scanning System) camera (Spectra Scan Model 704) from Photo Research Inc. In a typical measurement, 50–100 μL of a 1 mg mL^{-1} solution of the acridinium ester in a 2 : 1 mixture of water–MeCN (with 0.05% TFA) was diluted with 0.3 mL of reagent 1 comprising 0.5% hydrogen peroxide in 0.1 M nitric acid. Just prior to the addition of reagent 2 comprising 7 mM CTAC in 0.25 M sodium hydroxide, the shutter of the camera was opened and light was collected for 5 seconds. The output of the instrument is a graph of light intensity *versus* wavelength.

4. UV-Visible spectrophotometric measurements (Fig. 5 and Fig. S17–S20 ESI†)

UV-Visible spectrophotometry of acridinium esters **10a–10d** for determination of the pK_a of acridinium to pseudobase transition was carried out by dissolving the HPLC-purified acridinium esters in DMSO (~1 mg mL^{-1}). These solutions were further diluted 20-fold into 0.2 M phosphate buffer at pH 2, 2.6, 3.0,

Table 7 Acridinium ester label incorporation in protein conjugates

Protein/conjugate	Observed mass	Observed increase in mass	# Of labels
Unlabeled anti-TSH Mab	150 486	—	—
Anti-TSH Mab-**10a**	154 279	3793	4.2
Anti-TSH Mab-**10b**	155 419	4933	4.6
Anti-TSH Mab-**10c**	155 376	4890	4.3

3.5, 4.0, 4.5, 5.0, 5.5, 6.0, 6.5 and 7.0. A solution of 0.1 M HCl was used for pH 1. The diluted acridinium ester solutions were allowed to stand for one hour at room temperature and then UV-Visible spectra were recorded from 220–500 nm. The absorption intensity of the acridinium band at 371 nm for compound **10d** and 382–384 nm for compounds **10a–10c** was measured as a function of pH. A plot of this data is shown in Fig. 5. UV-Visible spectra of the acridinium esters **10a–10d** and their amine precursors **9a–9d** were also recorded in 0.1 M phosphate pH 2.8 and 0.1 M phosphate pH 9 respectively and are illustrated in Fig. S17–S20 (ESI†).

5. Chemiluminescence measurements (Tables 1–4, Fig. 6–9 and Fig. S21–S24 ESI†)

Chemiluminescence of acridinium esters **10a–10c** and their anti-TSH antibody conjugates was measured on an Autolumat LB953 Plus luminometer from Berthold Technologies. HPLC-purified acridinium esters **10a–10c** were initially dissolved in a mixture of methanol and 10 mM phosphate, pH 8 (1–2 mg mL^{-1}) and were further diluted for chemiluminescence measurements in an aqueous buffer, pH = 8, of 10 mM disodium hydrogen phosphate, 0.15 M NaCl, 8 mM sodium azide and 0.015 mM bovine serum albumin (BSA). Protein conjugates, 13–28 μM, based on protein concentration measured using the BCA protein assay from Pierce, were serially diluted 10^5-fold for chemiluminescence measurements. Similarly, solutions of acridinium ester labels (~0.5 mM) were serially diluted 10^6-fold for chemiluminescence measurements. A 0.010 mL volume of each diluted acridinium ester sample was dispensed into the bottom of a cuvette. Cuvettes were placed into the primed LB953 and the chemiluminescence reaction was initiated with the sequential addition of 0.3 mL of Reagent 1, a solution of 0.5% hydrogen peroxide in 0.1 M nitric acid followed by the addition of 0.3 mL of Reagent 2, a solution of 0.25 M sodium hydroxide with or without surfactant. Each chemiluminescence flash curve was measured in 240 intervals of 0.5 seconds (2 minutes total time) from the point of chemiluminescence initiation with the addition of 0.25 M NaOH. Each chemiluminescence reaction was carried out a minimum of three times, averaged and converted to a percentage of the chemiluminescence accumulated up to each time interval. Chemiluminescence values for 2 min collection times were also normalized for comparison to reactions without surfactant with reactions with the various surfactants. The output from the luminometer instrument was expressed as RLUs (relative light units). For evaluation of surfactants, the surfactant was either omitted or included in Reagent 2 with one of the following surfactants at five times its reported CMC in water: (a) cetyltrimethylammonium chloride (CTAC), CMC = 1.4 mM,[20] (b) cetyltripropylammonium chloride (CTPAC), CMC = 0.65 mM,[20] and (c) *N*,*N*-dimethyldodecylammonio-1,3-propane sulfonate (DDAPS), CMC = 3.17 mM.[21]

6. Micelle–water partition coefficients (Table 5 and Fig. S25–S31 ESI†)

Theory and experimental protocol for measurement of partition coefficients of acridinium esters to CTAC micelles is described in the ESI.† Partition coefficient plots of the acridinium esters are illustrated in Fig. S25–S31.

7. Measurement of chemiluminescence stability (Fig. 10)

Acridinium ester anti-TSH conjugates were diluted to a concentration of 0.2 nM in a buffer of 10 mM sodium phosphate, 8 mM sodium azide and 15 μM BSA at pH 8.0. The diluted conjugates were kept at 4 and 37 °C for four weeks. The residual chemiluminescence of each diluted conjugate was assessed over the course of the four weeks by periodically averaging the chemiluminescence measurements of five 10 μL samples on the Autolumat LB953 Plus luminometer with the change in chemiluminescence gauged against initial values as a percentage.

8. Measurement of non-specific binding (Table 6)

Acridinium ester anti-TSH conjugates were diluted to a concentration of 2 nM in a buffer of 0.1 M HEPES (4-(2-hydroxyethyl)-1-piperazineethanesulfonic acid), 0.15 M sodium chloride, 10 mM Triton-X100 and 0.1 mM BSA at pH 7.7. To 100 μL of each diluted conjugate was added and mixed, 200 μL of TSH-free serum and 0.25 mL of ADVIA:Centaur® (Siemens Healthcare Diagnostics) TSH3 assay solid phase containing magnetically separable, paramagnetic microparticles (PMPs) covalently derivatized with sheep anti-TSH polyclonal antibody. The mixed reagents were kept at room temperature for 15 min. The solid phase was magnetically collected and washed twice with 1 mL of water to remove unbound acridinium ester conjugate. Each test was carried out in sets of five replicates. The chemiluminescence of the washed magnetic particles was measured on the Autolumat LB953 Plus luminometer averaging the five replicate values. FNSB (fractional non-specific binding) was measured as the ratio of the chemiluminescence associated with the washed magnetic particles to the total chemiluminescence from 100 μL of each diluted conjugate mixed into the solid phase.

Acknowledgements

We thank Ms Yuanfang Deng for providing us with IR spectra of the synthetic compounds described in the manuscript.

References

1 (*a*) A. Natrajan, D. Sharpe, J. Costello and Q. Jiang, *Anal. Biochem.*, 2010, **406**, 204–213; (*b*) S.-J. Law, C. S. Leventis, A. Natrajan, Q. Jiang, P. B. Connolly, J. P. Kilroy, C. R. McCudden and S. M. Tirrell, *US Pat* 5 656 426, 1997; (*c*) A. Natrajan, D. Sharpe and Q. Jiang, *US Pat* 6 664 043 B2, 2003; (*d*) A. Natrajan, D. Sharpe and D. Wen, *Org. Biomol. Chem.*, 2011, **9**, 5092–5103.
2 (*a*) I. Weeks, I. Behesti, F. McCapra, A. K. Campbell and J. S. Woodhead, *Clin. Chem.*, 1983, **29** (8), 1474–1479; (*b*) P. W. Hammond, W. A. Wiese, A. A. Waldrop III, N. C. Nelson and L. J. Arnold Jr, *J. Biolumin. Chemilumin.*, 1991, **6**, 35–43.
3 (*a*) F. McCapra, *Acc. Chem. Res.*, 1976, **9** (6), 201–208; (*b*) F. McCapra, D. Watmore, F. Sumun, A. Patel, I. Beheshti, K. Ramakrishnan and J. Branson, *J. Biolumin. Chemilumin.*, 1989, **4**, 51–58.
4 (*a*) J. Rak, P. Skurski and J. Błażejowski, *J. Org. Chem.*, 1999, **64**, 3002–3008; (*b*) K. Krzymiński, A. Ożóg, P. Malecha, A. D. Roshal,

A. Wróblewska, B. Zadykowicz and J. Błażejowski, *J. Org. Chem.*, 2011, **76**, 1072–1085.
5 (*a*) J. Toullec and M. Moukawim, *Chem. Commun.*, 1996, 221–222; (*b*) V. K. Balakrishnan, E. Buncel and G. W. Vanloon, *Environ. Sci. Technol.*, 2005, **39**, 5824–5830; (*c*) C. A. Bunton and H. J. Foroudian, *Langmuir*, 1993, **9**, 2832–2835; (*d*) C. A. Bunton, M. M. Mhala, J. R. Moffat, D. Monarres and G. Savelli, *J. Org. Chem.*, 1984, **49**, 426–430.
6 (*a*) E. D. Hughes and C. K. Ingold, *J. Chem. Soc.*, 1935, 244–255; (*b*) E. D. Hughes, *Trans. Faraday Soc.*, 1941, **37**, 603–631; (*c*) E. D. Hughes and C. K. Ingold, *Trans. Faraday Soc.*, 1941, **37**, 657–685; (*d*) K. A. Cooper, M. L. Dhar, E. D. Hughes, C. K. Ingold, B. J. MacNulty and L. I. Woolf, *J. Chem. Soc.*, 1948, 2043–2049.
7 (*a*) P. D. Profio, R. Germani, G. Savelli, G. Cerichelli, N. Spreti and C. A. Bunton, *J. Chem. Soc., Perkin Trans. 2*, 1996, 1505–1509; (*b*) G. Cerichelli, L. Luchetti, G. Mancini, M. N. Muzzioli, R. Germani, P. P. Ponti, N. Spreti, G. Savelli and C. A. Bunton, *J. Chem. Soc., Perkin Trans. 2*, 1989, 1081–1085; (*c*) G. Cerichelli, G. Mancini, L. Luchetti, G. Savelli and C. A. Bunton, *J. Phys. Org. Chem.*, 1991, **4**, 71–76; (*d*) G. Cerichelli, L. Luchetti, G. Mancini, G. Savelli and C. A. Bunton, *Langmuir*, 1996, **12**, 2348–2352.
8 (*a*) L. Brinchi, P. D. Profio, R. Germani, G. Savelli and C. A. Bunton, *Langmuir*, 1997, **13**, 4583–4587; (*b*) L. Brinchi, R. Germani, G. Savelli, N. Spreti, R. Ruzziconi and C. A. Bunton, *Langmuir*, 1998, **14**, 2656–2662; (*c*) L. Brinchi, R. Germani, G. Savelli and C. A. Bunton, *J. Phys. Org. Chem.*, 1999, **12**, 890–894.
9 (*a*) C. A. Bunton and L. Sepulveda, *J. Phys. Chem.*, 1979, **83**, 680–683; (*b*) O. Duman, S. Tunç and B. Kanci, *Fluid Phase Equilib.*, 2011, **301**, 56–61; (*c*) M. F. Nazar, S. S. Shah and M. A. Khosa, *J. Surfactants Deterg.*, 2010, **13**, 529–537; (*d*) R. Hosseinzadeh, R. Maleki, A. A. Matin and Y. Nikkhahi, *Spectrochim. Acta, Part A*, 2008, **69**, 1183–1187.
10 (*a*) J. F. M. daSilva, S. J. Garden and A. C. Pinto, *J. Braz. Chem. Soc.*, 2001, **12**, 273–324; (*b*) A. Natrajan, Q. Jiang, D. Sharpe and J. Costello, *US Pat* 7 309 615 B2, 2007.
11 (*a*) O. Mitsunobu, *Synthesis*, 1981, 1–28; (*b*) D. L. Hughes, *Organic Reactions*, Wiley, New York, 1992, vol. 42, pp. 335–656.
12 A. Natrajan and D. Wen, *Green Chem.*, 2011, **13**, 913–921.
13 J. W. Bunting, V. S. F. Chew, S. B. Abhyankar and Y. Goda, *Can. J. Chem.*, 1984, **62**, 351–354.
14 (*a*) C. A. Bunton, F. Nome, F. H. Quina and L. S. Romsted, *Acc. Chem. Res.*, 1991, **24**, 357–364; (*b*) P. Scrimin, P. Tecilla, U. Tonellato and C. A. Bunton, *Colloids Surf., A*, 1998, **144**, 71–79; (*c*) L. S. Romsted, C. A. Bunton and J. Yao, *Curr. Opin. Colloid Interface Sci.*, 1997, **2**, 622–628.
15 (*a*) C. A. Bunton, M. M. Mhala and J. R. Moffat, *J. Org. Chem.*, 1987, **52**, 3832–3835; (*b*) A. Natrajan and C. N. Sukenik, *J. Org. Chem.*, 1988, **53**, 3559–3563.
16 H. Gharibi, B. M. Razavizadeh and M. Hashemianzaheh, *Colloids Surf., A*, 2000, **174**, 375–386.
17 D. W. Armstrong and F. Nome, *Anal. Chem.*, 1981, **53**, 1662–1666.
18 S.-J. Law, T. Miller, U. Piran, C. Klukas, S. Chang and J. Unger, *J. Biolumin. Chemilumin.*, 1989, **4**, 88–98.
19 (*a*) R. C. Chapman, E. Ostuni, L. Yan and G. M. Whitesides, *Langmuir*, 2000, **16**, 6927–6936; (*b*) R. C. Chapman, E. Ostuni, M. N. Liang, G. Meluleni, E. Kim, L. Yan, G. Pier, H. S. Warren and G. M. Whitesides, *Langmuir*, 2001, **17**, 1225–1233; (*c*) S. J. Sofia, V. Premnath and E. W. Merrill, *Macromolecules*, 1998, **31**, 5059–5070; (*d*) Y.-H. Zhao, B.-K. Zhu, L. Kong and Y.-Y. Xu, *Langmuir*, 2007, **23**, 5779–5786; (*e*) A. R. Denes, E. B. Somers, A. C. L. Wong and F. Denes, *J. Appl. Polym. Sci.*, 2001, **81**, 3425–3438; (*f*) J. Ladd, Z. Zhang, S. Chen, J. C. Hower and S. Jiang, *Biomacromolecules*, 2008, **9**, 1357–1361; (*g*) Y. Chang, S. Chen, Z. Zhang and S. Jiang, *Langmuir*, 2006, **22**, 2222–2226; (*h*) Z. Zhang, T. Chao, S. Chen and S. Jiang, *Langmuir*, 2006, **22**, 10072–10077; (*i*) W. K. Cho, B. Kong and I. S. Choi, *Langmuir*, 2007, **23**, 5678–5682; (*j*) G. Cheng, Z. Zhang, S. Chen, J. D. Bryers and S. Jiang, *Biomaterials*, 2007, **28**, 4192–4199; (*k*) H. Kitano, A. Kawasaki, H. Kawasaki and S. Morokoshi, *J. Colloid Interface Sci.*, 2005, **282**, 340–348.
20 R. Bacaloglu, C. A. Bunton and F. Ortega, *J. Phys. Chem.*, 1989, **93**, 1497–1502.
21 Y. Wang, X. Huang, Y. Li, J. Wang and Y. Wang, *Colloids Surf., A*, 2009, **333**, 108–114.
22 D. W. Armstrong and G. Y. Stine, *J. Am. Chem. Soc.*, 1983, **105**, 2962–2964.
23 A. Berthod, *J. Chromatogr., A*, 1997, **780**, 191–206.
24 M. Arunyanart and L. J. Cline Love, *Anal. Chem.*, 1984, **56**, 1557–1561.